令和元年度　博士論文

Organic Matter Decomposition by In-liquid Plasma

液中プラズマによる有機物分解

愛媛大学大学院生産環境工学専攻

丹下　和樹

Contents

Chapter 1. General introduction

1 – 1 Background of this study

Plasma is a state in which the molecules that make up a gas are ionized and divide into cations and electrons, and are generated by heating the gas or by a strong magnetic field and electric field. Industrial applications of plasma include plasma displays, thin film synthesis, etching, and fluorescent lamps, which are applied in a very wide range of fields.

In-liquid plasma is a technology that generates plasma in a liquid, and radicals, electrons, and ultraviolet rays that exist in the plasma can act on the liquid. Most of the technology for generating plasma in liquids used pulsed high voltage, but in the 2000s, plasma generation technology in water using high frequency and microwave was devised [1,2]. The high-frequency plasma generator includes an electromagnetic wave oscillator and electrodes. For example, when a metal electrode is irradiated with a high frequency, the electrode is heated, bubbles are generated from the electrode tip, and then plasma is generated from the electrode tip. Since the plasma impedance varies greatly before and after plasma generation, it is important to match impedance before and after generation. If matching is good, plasma can be easily generated in the liquid.

Research on the application of this plasma generation method has been actively conducted. Mg(OH)2, Zn/ZnO, WO_3 and Ag nanoparticles were synthesized from submerged magnesium, zinc, and silver rods [3–6]. This method does not use chemicals required for chemical synthesis, which is a general nanoparticle synthesis method, and has the advantage of not discharging waste liquid into the environment. It was also reported that metal oxide powder dispersed in alcohol was reduced by in-liquid plasma [7,8].

Research is also underway to produce useful energy such as hydrogen by decomposing biomass and waste using plasma in liquid. It has been reported that the efficiency of hydrogen production was

improved by generating high-frequency plasma in an aqueous glucose solution compared to when pure water was decomposed [9]. Generally, a biomass drying process is required to use biomass as an energy source, but it can be used in a wet state with the In-liquid plasma. It was reported that plasma is generated even in nonpolar solutions, and hydrogen can be generated by decomposing dodecane and waste oil [10]. However, the amount of hydrogen production per input power was less than or almost equal to that of water electrolysis. In recent years, attempts was made to combine steam reforming and catalysts with plasma in order to achieve hydrogen generation efficiency higher than electrolysis of water [11,12]. They have achieved efficiencies that exceed electrolysis, but have a cost problem due to the use of liquid fuel as raw material. From now on, research focusing on further improvement of efficiency and the simultaneous generation of valuable materials is expected.

1 – 2 Motivation of this study

Since 1970, human resource demand for nature for one year has been increasing beyond the regenerative capacity of the earth. In 2008, to continue to use human resources, it will be necessary to have a regeneration capacity equivalent to 1.5 Earths, and in 2030 it is expected to require 2 Earths [13]. Carbon dioxide emissions from the use of fossil fuels are a major factor in this problem. The importance of technologies that use biomass and waste as energy resources is increasing as the serious impact of greenhouse gases on the earth is advancing rapidly.

Non-food crops such as rice straw and rice husks and some of the forest remaining wood are used as compost and fuel, but most are not used effectively. These are mainly composed of cellulose, hemicellulose, and lignin, and their strong binding makes it difficult to use as an energy resource. Research into the process of converting cellulose to saccharides has been conducted [14]. Well-known saccharification methods include acid hydrolysis and enzyme hydrolysis [15,16]. The acid saccharification method has the advantage of a high reaction rate, but there are problems of overdegradation of the product and the environmental load due to the need for waste liquid treatment. Concentrated acid hydrolysis is expensive because it requires a large amount of acid, and acid recycling

is quite expensive [17]. On the other hand, in the enzymatic saccharification method, the reaction rate is slow, but the excessive decomposition does not proceed. However, pretreatment is necessary and the cost of enzymes is a problem for practical use [18–21]. In recent years, ultrasonic welding was applied to cellulose degradation as a new alternative method, and sugar conversion using hydrolysis and thermal decomposition caused by frictional heat was attempted. Cellulose in the filter paper was decomposed into 5-hydroxymethylfurfural (5-HMF), furfural, and oligosaccharide through hydrolysis and thermolysis that occurs in the welding process [22]. Many methods using supercritical water have been reported, and biomass was converted into useful gases such as hydrogen. [23–25].

The solvents used by factories and research institutes are discarded, but most of them are treated by the combustion method and release carbon dioxide. The waste solution contains volatile organic compounds (VOCs) such as acetone and toluene. VOCs harm human beings (carcinogenic effects, nervous system paralysis, anxiety, etc.) and environments (ozone holes, global warming, etc.) [26,27]. For this reason, various technologies for VOCs removal have been studied, and treatments such as thermal oxidation [28–31], biological filtration [32–34], adsorption [35,36], and aggregation are performed.

Most of the chemical substances that are the raw materials for producing chemical products and synthesis gas (hydrogen + carbon monoxide) are generated from fossil fuels such as coal and petroleum. If the raw material can be replaced with biomass from fossil fuel, a carbon neutral and sustainable society will be realized. At the same time, it is important to use wastes such as waste solvents as raw materials for energy such as hydrogen and carbon materials.

The purpose of this research is to adapt in-liquid plasma to decomposition of biomass and waste solvent. Regarding the decomposition of biomass, research was reported in which plasma was generated in a cellulose dispersion [9]. However, the type of solution was not mentioned, and the relationship with each parameter such as plasma temperature and plasma size was unknown. The effect of the electrolytic solution on cellulose decomposition was investigated by comparing the gas production rate and plasma parameters. This is explained in Chapters 2 and 3. In Chapter 4, lignin, another major component of woody biomass, was decomposed. In addition to the product gas, the decomposition products dissolved

in the liquid were qualitatively and quantitatively determined. In Chapter 5, acetone was decomposed by plasma in liquid as a model of waste solvent. The product and its decomposition mechanism were investigated in detail. Chapter 6 outlines these studies.

Chapter 2. Effect of Pretreatment by Sulfuric Acid on Cellulose Decomposition Using the In-Liquid Plasma Method

2 – 1 Introduction

Currently many researchers are working to develop clean and renewable alternative energy sources due to the reduction of fossil fuels reserves, the serious damage from greenhouse gases (GHGs) and the rapid growing of worldwide energy needs [37–40]. Hydrogen energy is the most promising energy carrier for sustainable development. The dominant benefits of hydrogen as an alternative energy carrier consist of reduction of global greenhouse gas emission, reduction of urban air pollutants, security of energy supply through the diversification of energy production and increase in the efficiency of hydrogen fuel cell technology [41]. If hydrogen energy is to be considered as the clean energy source for the future, a novel generation technology will be necessary to meet the increase in demand.

Biomass is the first- fuel ever used by humankind and one of the most abundant renewable resources in the world contributing about 10 to 15% of today's world energy demand [42]. Biomass is versatile fuel that can be the source of biogas, liquid fuels and electricity. Biomass energy is carbon neutral in that it is derived from plants, a stored source of solar energy in the form of chemical energy through the process of photosynthesis [43]. It can be released when the chemical bonds between adjacent carbon, hydrogen and oxygen molecules are broken by various thermo-chemical and biological energy conversion processes [44]. The conversion of plant material into a suitable form of energy, for instance, electricity or fuel can be achieved using a number of various routes [45]. Pyrolysis and gasification of renewable biomass energy have been found to be the most favorable thermo-chemical conversion processes for hydrogen production [46]. It was found that conventional pyrolysis and gasification produces not only useful fuel gases, char and chemicals but also byproducts such as fly ash, NO_x, SO_2 and tar [47]. This leads to severe operational problems such as clogging and blockage in fuel lines, filters

and engines when the tar in the product gases condenses at low temperatures. Hence, the investigation of new processes that can reduce the production of tar is of utmost importance.

Plasma is a clean technique that has great application potential for treating various types of hazardous wastes [48]. It is a more or less ionized produced gas mainly by electric fields, which consist of a mixture electrons, ions, neutral particles and so on [49]. Plasma enhances chemical reaction rates since in plasma it is possible to instantaneously form strong radical species such as H, O, OH, HO_2, etc [50,51]. The formation of UV radiation in plasma discharge also has been suggested to be a cause of effective degradation [52]. Among the plasma discharge processes, radio-frequency (RF) plasma in liquid has great potential, but until recently has received little attention for biomass conversion. With this method, the low liquid temperatures and high molecular density of liquid in comparison to those of gases provide great appeal for application in low-temperature environments and to generate higher reaction rates [10,53]. The electron temperature of RF in-liquid plasma is estimated to be in the range between 3300 and 4800 K [54]. Since cellulose, one of the basic constituents in biomass, is nonvolatile, it cannot enter the bubbles containing plasma. With the application of in-liquid plasma, the cellulose is not directly decomposed by the plasma, but rather is decomposed indirectly by the active radicals created by the plasma [9].

The purpose of this research is to convert cellulose in electrolyte solution into hydrogen gas by using RF in-liquid plasma. The conductivity of solutions is important parameter for in-liquid plasma. The size of plasma increases with conductivity because it leads to a reduction of RF power loss in water. The decomposition efficiency of the organic matter by in-liquid plasma changes depending on the conductivity of solutions [55]. Some electrolytic solutions such as 1 mol/dm^3 NaOH containing many OH^- ions, 1 mol/dm^3 H_2SO_4 containing many H^+ ions, and 0.333 mol/dm^3 Na_2SO_4 containing many Na^+ ions and SO_4^{2-} ions were used as the solvents of cellulose to promote the reaction for cellulose decomposition.

2 – 2 Experimental method

A schematic diagram of apparatus for decomposition of a cellulose suspension is shown in Fig. 2-1. A 3.0 mm diameter copper electrode was inserted vertically from the bottom of reactor. An aluminum tube, used as a dielectric substance to avoid energy loss, enveloped the electrode. A counter electrode was attached to the top of the reactor and fixed at 26.0 mm from the tip of the copper electrode.

The experimental procedures were as follows. Initially, the pressure of the reactor was reduced to 0.01-0.02 MPa using an aspirator. In this condition, power input from a 27.12 MHz radio-frequency (RF) generator and impedance were simultaneously adjusted by a matching box. Plasma was discharged at the tip of electrode instantly after electric breakdown. The discharge power was 150 W and the AC voltage was 200 V, as calculated by subtraction of the reflected power from the input power.

In this experiment, the three solutions used as a reagent were 1 mol/dm^3 H_2SO_4, 1 mol/dm^3 NaOH and 0.333 mol/dm^3 Na_2SO_4. Pure water was used as a control reagent. These reagents were used to enhance

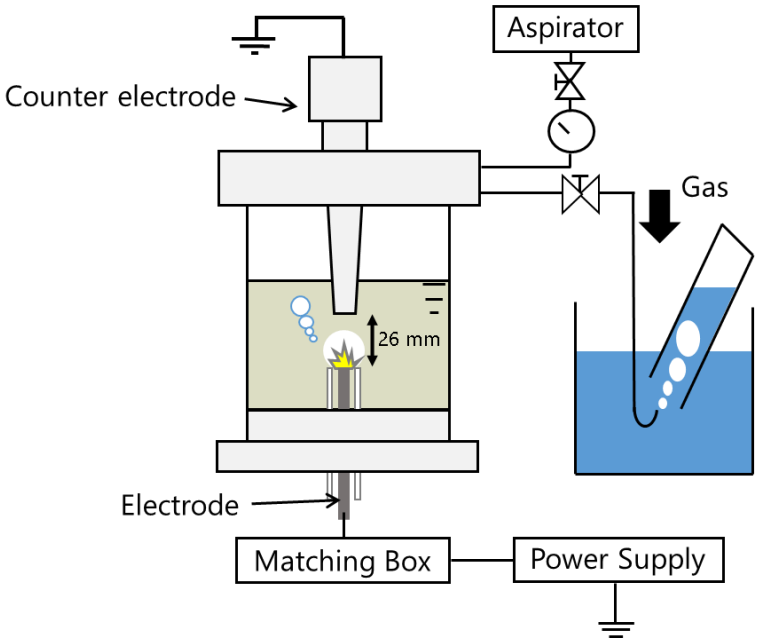

Fig. 2-1. Experimental set-up.

the gas production rate from decomposition of cellulose suspension by RF in-liquid plasma. Cellulose powder passed through a 38.0 μm mesh (catalogue number 034-22221) provided by Wako Pure Chemical Industries, Japan was employed as the source material. The experiments were performed at initial cellulose contents of 0.5, 10.0 and 20.0 wt%.

The pressure increased due to the gas generation and reached atmospheric pressure. Then the produced gas was drawn out of the apparatus by an air-tight glass syringe. The gas production rate was measured at one minute intervals. Then, the produced gas was analyzed using a gas chromatograph (GC-8A Shimadzu). Argon was used as the carrier gas.

2 – 3 Results and Discussion

2 - 3 - 1 Gas production rate and composition

As a preliminary study, gas production from a cellulose suspension decomposed by RF in-liquid plasma using 0.333 mol/dm^3 Na_2SO_4 reagent was compared to that employing pure water. As shown in Fig. 2-2, with 0.333 mol/dm^3 Na_2SO_4 the gas production rate was increased by a maximum of 5 times in comparison to that using pure water at an initial cellulose content of 20.0 wt%. The decomposition of cellulose will not occur directly by the plasma, because cellulose is nonvolatile. OH radicals are produced in the plasma via the decomposition of water molecules [55]. It is assumed that OH radicals decompose cellulose by strong oxidation power. When pure water was used and the content of cellulose was 10.0 wt%, the gas production rate was found to be lower than when 0.5wt% of cellulose was used. It is thought that the cellulose might act to prevent the decomposition of water. The evaporated water is fed into the plasma, and decomposed by the plasma. The amount of the evaporation is reduced by the cellulose covering the surface of the bubble, and thus the production rate decreases with an increase of the cellulose concentration [9]. When the content of cellulose was 20.0 wt%, it is assumed that the decomposition of cellulose occurred easily due to probability of cellulose existing near plasma increased. When 0.333 mol/dm^3 Na_2SO_4 is used as a reagent, the gas production rate increased as the initial cellulose content increases. The conductivity of 0.333 mol/dm^3 Na_2SO_4 is higher than pure water and

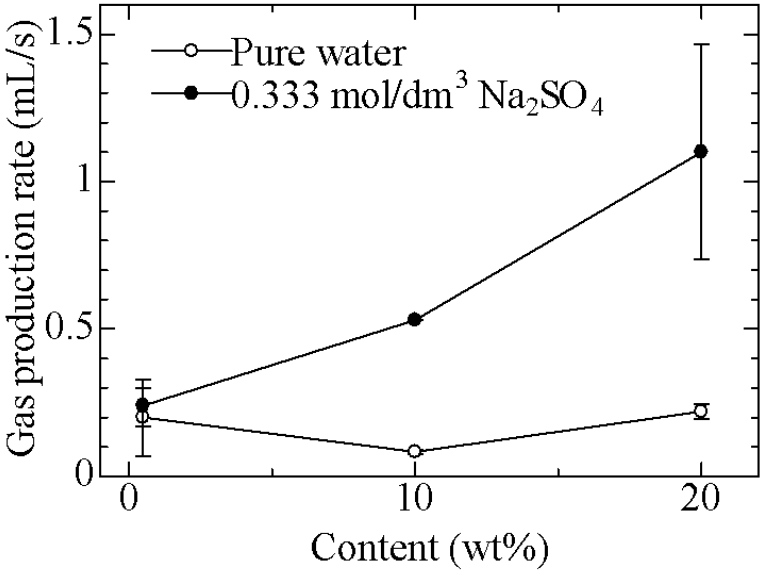

Fig. 2-2. Gas production rate by cellulose content.

RF power loss is low. So, plasma was generated efficiently.

The experiment was then conducted at an initial cellulose content of 20.0 wt% employing various types of reagents. Fig. 2-3 shows the rate of produced gas from decomposition of cellulose suspensions at an initial cellulose content of 20.0 wt% employing pure water, 0.333 mol/dm^3 Na_2SO_4, 1 mol/dm^3 H_2SO_4 and 1 mol/dm^3 NaOH as reagents. As can be seen in figure, employing reagents for cellulose decomposition enhanced the gas production rate compared to pure water. The effects of 1 mol/dm^3 H_2SO_4 and 0.333 mol/dm^3 Na_2SO_4 reagents on gas production rate are less significant in comparison to 1 mol/dm^3 NaOH reagent. However, when 1 mol/dm^3 NaOH reagent was used, the gas production rate dropped over time. Decomposition using 1 mol/dm^3 NaOH as a reagent had a significant effect on the gas production rate. Here, since the 0.333 mol/dm^3 Na_2SO_4 was used in present study, if molar concentration increases, the gas production rate may be enhanced. The molarity of solutions is a topic of future discussion.

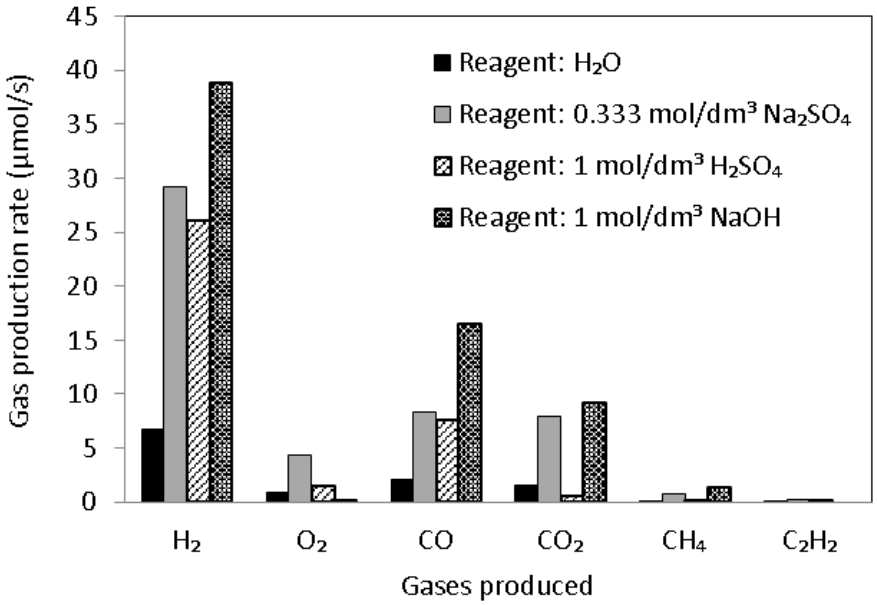

Fig. 2-4. Gas production rate at an initial cellulose content of 20 wt%. The rate of gas is an average for 20min after atmospheric pressure is obtained.

The gas production rates from decomposition of cellulose suspensions by RF in-liquid plasma in various types of reagents at an initial cellulose content of 20.0 wt% are shown in Fig. 2-4. The rate of gas is an average for 20.0 min after atmospheric pressure is obtained. By using 1 mol/dm^3 NaOH as a reagent, the hydrogen production rate was 6 times as high as that of pure water.

0.333 mol/dm^3 Na_2SO_4 and 1 mol/dm^3 H_2SO_4 reagents were 4 times as high as that of pure water. However, utilization of reagents for the decomposition of cellulose suspension leads to formation of some unwanted byproducts such as carbon monoxide (CO) and carbon dioxide (CO_2). The amount of methane (CH_4) and acetylene (C_2H_2) produced can be neglected due to their too small amounts.

2 - 3 - 2 Energy efficiency in hydrogen production

EPR (energy payback ratio) was measured in order to define economical production of H_2. Equation (1) shows the calculation of EPR:

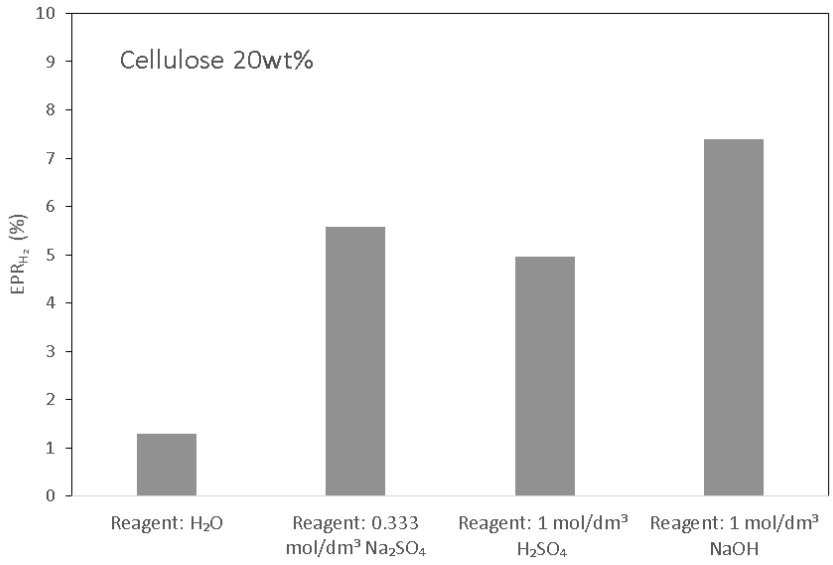

Fig. 2-5. Gas production rate for each solvent at an initial cellulosecontent of 20 wt%.

$$\mathrm{EPR}_{H2} = \frac{n_{H_2} \times \Delta H_{H_2}}{P} \times 100(\%) \quad (1)$$

n_{H_2} is the gas production rate of H_2 (mol/s), ΔH_{H_2} is the standard heat of combustion of H_2 (J/mol), and P is the input pour (W). The rate of gas is an average for 20 min after atmospheric pressure is obtained. The EPR_{H2} from decomposition of cellulose suspensions by RF in-liquid plasma in various types of reagents at an initial cellulose content of 20 wt% is shown in Fig 2-5. The highest EPR_{H2} was obtained when using 1 mol/dm^3 NaOH, then decreased in the order, 0.333 mol/dm^3 Na_2SO_4, 1 mol/dm^3 H_2SO_4, with the lowest case being pure water.

2 - 3 - 3 Relationship between hydrogen production rate and cellulose gasification

A well-known property of cellulose is that, by itself, it is insoluble in water due to the multiplicity and strength of the hydrogen bonds formed between cellulose chains in fibrils. It is these intra- and intermolecular hydrogen bonds that make cellulose insoluble in water. By using NaOH, He et al. proved that NaOH was capable of breaking some intra- and intermolecular hydrogen bonds through

complex reaction [56]. Thus it was expected that using 1 mol/dm^3 NaOH would lead to the degradation of cellulose and make cellulose more susceptible to be attacked by radical species produced from RF in-liquid plasma compared to using 1 mol/dm^3 H_2SO_4 and 0.333 mol/dm^3 Na_2SO_4. The radical species produced by RF in-liquid plasma includes OH, H and O atoms [2,57].

In order to determine the degree of decomposition of cellulose suspension, the carbon gasification rate were measured. The rate is an average for 20.0 min after atmospheric pressure is obtained. The carbon gasification was determined by the total number of C atoms produced as carbon monoxide (CO), carbon dioxide (CO_2), methane (CH_4) and acetylene (C_2H_2). Fig 2-6 shows the carbon gasification rate through the decomposition process of cellulose in pure water, 0.333 mol/dm^3 Na_2SO_4, 1 mol/dm^3 H_2SO_4 and 1 mol/dm^3 NaOH reagents. The amount of C atoms produced during decomposition of cellulose suspension using 1 mol/dm^3 NaOH reagent was 7 times higher than that of pure water alone. The rates for 0.333 mol/dm^3 Na_2SO_4 and 1 mol/dm^3 H_2SO_4 reagents were only 4.5 times and 2.3 times higher than that of pure water, respectively. This shows that carbon gasification rate of cellulose suspension in 1 mol/dm^3 NaOH reagent is higher than the others.

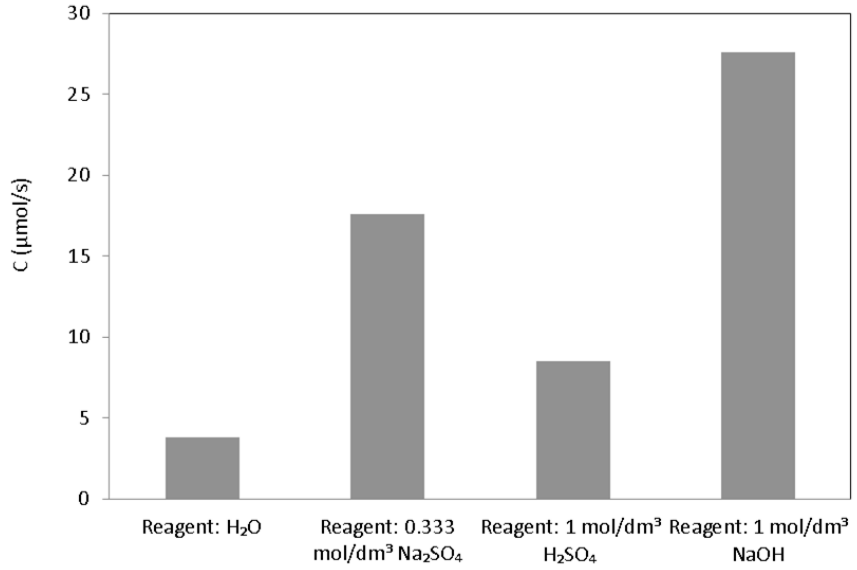

Fig. 2-6. Carbon gasification rate at an initial cellulose content of 20 wt%. The carbon gasification rate is an average for 20min after atmospheric pressure is obtained.

Fig 2-7 shows the relationship between the hydrogen production rate and the quantity of carbon atom in the product gas. The hydrogen production rate tends to rise as the quantity of carbon atoms in the product gas rise. This result suggests that a greater amount of hydrogen can be obtained by the gasification of cellulose with in-liquid plasma.

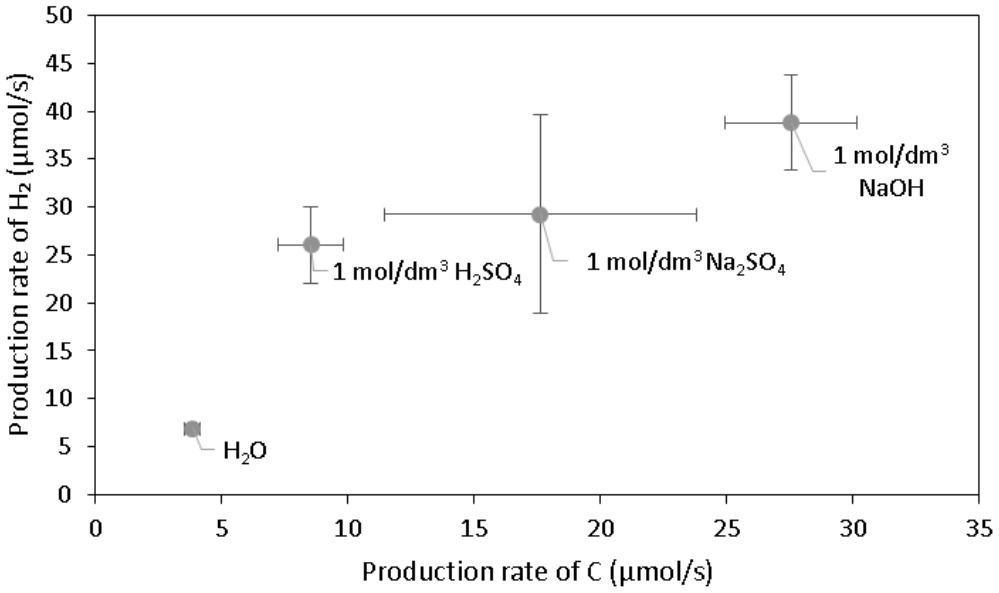

Fig. 2-7. The relationship between the hydrogen production rate and the quantity of carbon atom in the product gas. Here, the error bar shows all experimental data.

2 – 4 Conclusion

Decomposition of cellulose suspension in liquids, such as 1 mol/dm^3 NaOH, 1 mol/dm^3 H_2SO_4, 0.333 mol/dm^3 Na_2SO_4 and pure water, was carried out using 27.12MHz in-liquid plasma and the gas production rates were measured. When 0.333 mol/dm^3 Na_2SO_4 is employed, the gas production rate by in-liquid plasma was enhanced as the initial cellulose content was increased. The highest hydrogen production rate was obtained when using 1 mol/dm^3 NaOH, then decreased in the order, 0.333 mol/dm^3 Na_2SO_4, 1 mol/dm^3 H_2SO_4, with the lowest case being pure water. The hydrogen production rate from 1 mol/dm^3 NaOH was increased by 7 times over that from pure water. The highest EPR_{H2} was obtained when using 1 mol/dm^3 NaOH, then decreased in the order, 0.333 mol/dm^3 Na_2SO_4, 1 mol/dm3 H_2SO_4, with the lowest case being pure water. The hydrogen production rate tends to rise as the quantity of carbon atoms in the product gas rise.o enhance hydrogen productio efficiency, catalytic effects have been investigated for the in-liquid plasma metod of methanol decomposition.

Chapter 3. Cellulose Decomposition in Electrolytic Solution Using In-Liquid Plasma Method

3 – 1 Introduction

Biomass is one of the most abundant renewable resources that currently provides approximately 10%–15% of the world's energy demand [42] and is a versatile fuel that can be processed to produce biogas, liquid fuels, and electricity [58,59]. Furthermore, energy derived from biomass is carbon neutral because it is derived from plants, which convert solar energy and carbon sources to chemical energy through photosynthesis [43]. Cellulose is expected to be utilized as a major component of renewable resources because it cannot be used as a food source. However, the molecular structure of cellulose, (1→ 4)β-D-glucan, allows strong inter- and intramolecular H_2 bonds to form between chains, which makes any efforts to process or modify the material exceeding difficult [60,61].

The purpose of this research is to convert cellulose into fuel. One effective method of treating waste materials and organic matter is to use the highly active energy field of plasma [62–65]. Gao et al. preformed deconstruction of lignocellulosic biomass in a hydrogen background gas by using low temperature plasma. They indicated that low temperature plasma can open pathways in the conversion of lignocellulosic biomass to products not observed in conventional thermochemical processing [66]. The authors have previously developed a method to produce H_2 from cellulose by using "in-liquid plasma", in which gas bubbles are formed in liquids under high pressure; thus, a chemical reaction field that reaches 3500 K is created [67,68]. Plasma is generated by applying radio frequency (RF) and microwave radiation [1,2,69,70]. This method allows direct decomposition of harmful substances without a catalyst. Previous reports in the literature have also described the use of in-liquid plasma decomposition for H_2 production; several of these reports use organic solvents as the starting material

[10,71–73]. Ultimately, the goal is to produce H_2 efficiently because H_2 is expected to be an important energy source [73,74]. Current commercial production of hydrogen gas is conducted using the methane steam reforming method [75–77]. Many scientists are working in an improvement of H_2 generation method [78–81].

The decomposition of cellulose suspensions for H_2 production by using in-liquid plasma at 27.12 MHz was described in previous studies [57,82]. In this method, the drying process of cellulose is not needed and radical species having strong oxidation power are generated from the decomposition of water [51]. H_2, O_2, CO, CO_2, and CH_4 are produced by decomposing cellulose suspension. In addition, it was found that some electrolytic solutions, such as those containing NaOH, H_2SO_4, and Na_2SO_4, can enhance the rate of gas production from a cellulose suspension [83]. However, the reason for this has yet to be completely understood. This study evaluates the production rates of gases from the decomposition of a cellulose suspension in 0.01 to 1.00 mol/dm^3 Na_2SO_4 and pure water by using 27.12-MHz in-liquid plasma. The concentration of Na_2SO_4 is observed to affect plasma size, gas temperatures, and •OH emission. The results of this experiment will provide useful knowledge about the effect of electrolytes on the decomposition of cellulose suspensions by in-liquid plasma.

3 – 2 Experimental material and methods

A schematic diagram of the apparatus for decomposition of a cellulose suspension is shown in Fig. 3-1. About 120 cm^3 of cellulose solution at 40 °C was placed in the reactor. As a visual window, a polycarbonate container with an interior diameter of 55 mm, an exterior diameter of 60 mm and a height of 90 mm was used in the reactor. A copper electrode with a 3.0-mm diameter is inserted vertically from the bottom of the reactor and enveloped by a quartz glass tube, which is a dielectric substance, to minimize energy loss. The bottom of the reactor is composed of copper and acts as the counter electrode.

In this experiment, 0.01 to 1.00 mol/dm^3 Na_2SO_4 and pure water were the reagents. Na_2SO_4 was used to enhance the gas production rate resulting from the decomposition of the cellulose suspension by RF

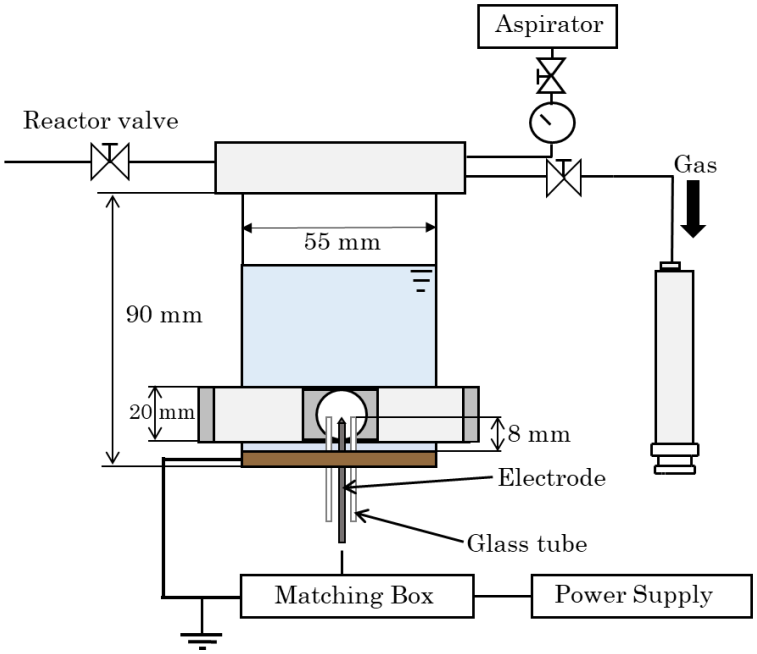

Fig. 3-1. Experimental set-up for the decomposition of a cellulose suspension.

in-liquid plasma. The source material was cellulose powder $(C_6H_{10}O_5)_n$ and filtered using a 38.0-μm mesh (Cat No. 034-22221, Wako Pure Chemical Industries, Japan). The experiments were performed with initial cellulose contents at 0.0 and 20.0 wt%. Photographs of cellulose powder and 20 wt% cellulose solution are shown in Fig. 3-2.

The experimental procedures are as follows. The pressure of the reactor was first reduced to be between 0.0050 and 0.0075 MPa by using an aspirator. Under this condition, power input from a 27.12-MHz RF generator and impedance were simultaneously adjusted using a matching box. The discharge power was 200 W and the AC voltage was 200 V, both of which were calculated by subtracting the reflected power from the input power. Subsequently, the reactor valve was opened to raise the reactor pressure to atmospheric pressure. The produced gases of 90 mL were sampled by an air-tight glass syringe 90 second after plasma irradiation. The gas production rate is calculated based on the time needed for obtaining the volume of a 90 ml syringe. After plasma irradiation for 8 minutes, the cellulose powder was removed by centrifugation, and the supernatant solution was analyzed.

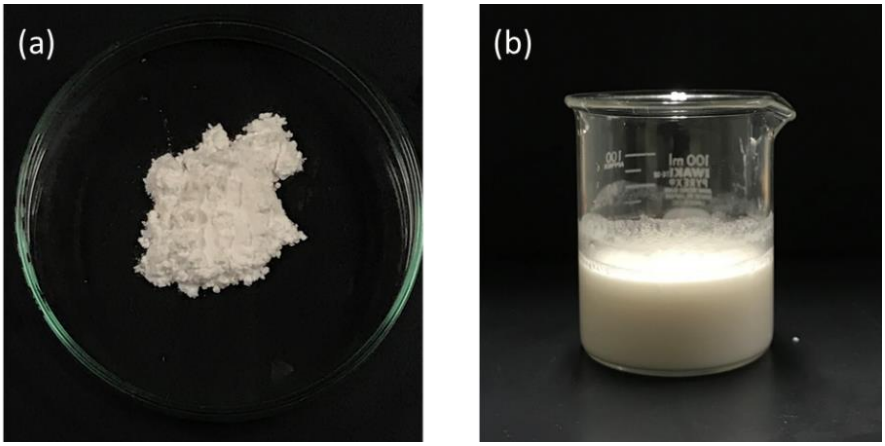

Fig. 3-2. Experimental set-up for the decomposition of a cellulose suspension.

A Shimadzu GC-8A instrument was used to analyze the produced gases. The column used was a SHIMADZU GC Stainless Column SHINCARBON ST (length, 4 m; diameter, 3 mm). The temperature was controlled from 60 °C for 6.0 min to 160 °C at a rate of 10.0 °C/min and it was held at 160 °C for 14 min. An argon carrier gas was applied at a flow rate of 50 mL/min. The produced gases were identified based on their retention times compared with those of authentic gases.

Shimadzu GCMS-QP2010 Ultra and GC-2010 Plus instruments were used to analyze the solution. The capillary column was a Rxi-1 ms column (length, 30 m; diameter, 0.25 mm; thickness, 0.25 μm). The temperature was controlled from 50 °C for 5.0 min to 250 °C at a rate of 10.0 °C/min and it was held at 250 °C for 10 min. A helium carrier gas was applied at a flow rate of 1.9 mL/min. The injector temperature was 230 °C. One microliter of the solution was directly injected.

Two spectroscopic measurement systems were used in this study. Light from plasma was guided through a quartz window to a spectrometer. The quartz window (thickness: 5 mm) was mounted at the side of the reactor and fixed using an acrylic cap, while the optical fiber was mounted in front of the quartz window. The first system comprised a photonic multichannel analyzer (PMA-11, HAMAMATSU); in this system, the measured spectrum ranged from 200 to 950 nm. The second system comprised a high-resolution spectrometer Ocean Optics HR 4000 (280–330 nm, 2400 groovesmm^{-1}, wavelength resolution of 0.06 nm); this was used to measure the spectral lines of •OH. In this study, the

coordinates of the electrode and the spectrometer were fixed. The emission intensity obtained by the spectroscope was used.

3– 3 Results and discussion

3- 3 - 1 Gas productions rate and gas composition

The gas productions rates from the cellulose suspensions and the solution without cellulose (only solution) that have been decomposed by RF in-liquid plasma are shown in Fig. 3-3. It was found that the gas productions rates increased with the concentration of Na_2SO_4. A comparison between the cellulose suspensions versus only solution revealed that the gas productions rate of the cellulose suspensions was higher than that of the solution without cellulose.

The composition of gas products produced and their yields are shown in Fig. 3-4. The definition of gas yield is the molar ratio to the total gas produced. Fig. 3-4(a) shows that O_2 and H_2 were generated from

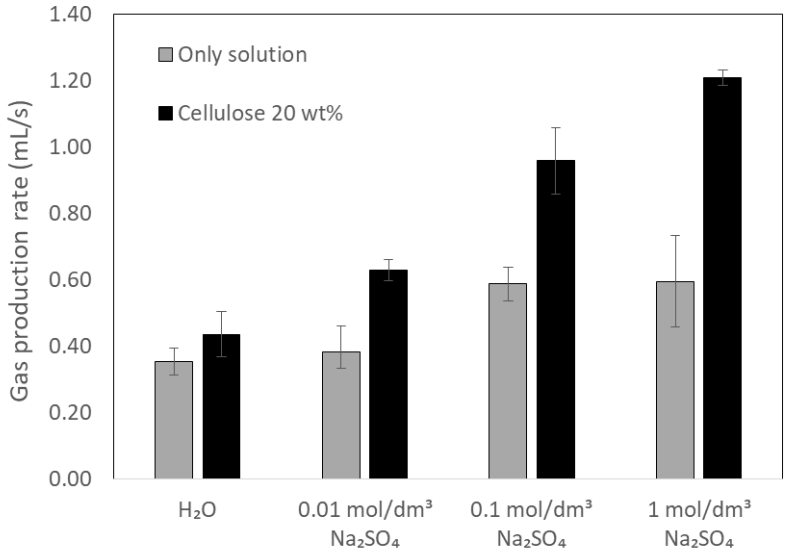

Fig. 3-3. Gas production rate versus Na_2SO_4 concentration.

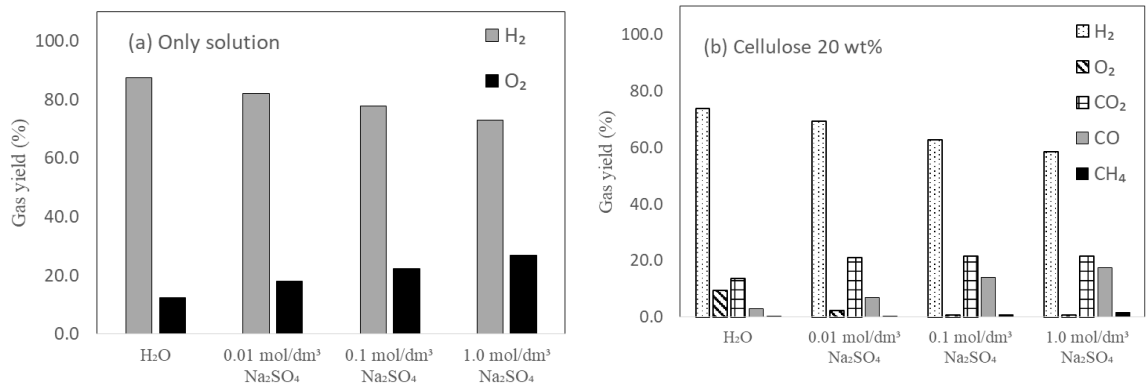

Fig. 3-4. Gas productions types and percentages for (a) without cellulose and (b) cellulose 20 wt%.

solution without cellulose. Moreover, the O_2 percentage increased with an increase in the concentration of Na_2SO_4. This suggests that oxygen was generated by decomposition of Na_2SO_4. Fig. 3-4(b) shows that O_2, H2, CO, CO_2, and CH_4 were generated from the cellulose suspensions. The productions of CO, CO_2, and CH_4 suggest that cellulose gasification occurred. The percentages of these gases increased with concentration of Na_2SO_4, suggesting that Na_2SO_4 concentration influences the efficiency of cellulose gasification.

3- 3 - 2 Plasma size and gas temperature

Since the plasma emission generated in the cellulose solution is absorbed by cellulose powder, it cannot be confirmed. Therefore, the spectroscopic and photographic data shown below is a cellulose-free solution. The spectral lines from the plasma are shown in Fig. 3-5. Fig. 3-5(a) shows the spectrum of the RF plasma in pure water. Emission lines from OH, sodium, hydrogen and oxygen are observed. The source of sodium emission is Sodium that is contained in the glass tube covering the electrode. Fig. 3-5(b) shows the spectrum of the RF plasma in 1 mol/dm^3 Na_2SO_4 solution. A strong Na-D line is observed along with emission lines from OH and hydrogen. Photographs were used to estimate the plasma size (Fig. 3-6). To avoid overexposure due to the bright shine of sodium ions (Na^+) and subsequent

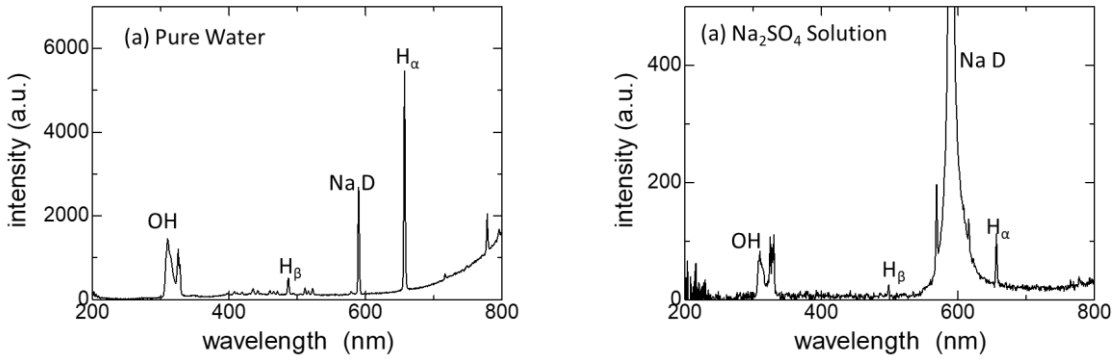

Fig. 3-5. Emission spectrum of RF plasma generated in (a) pure water and (b) 1 mol/dm^3 Na_2SO_4 solution.

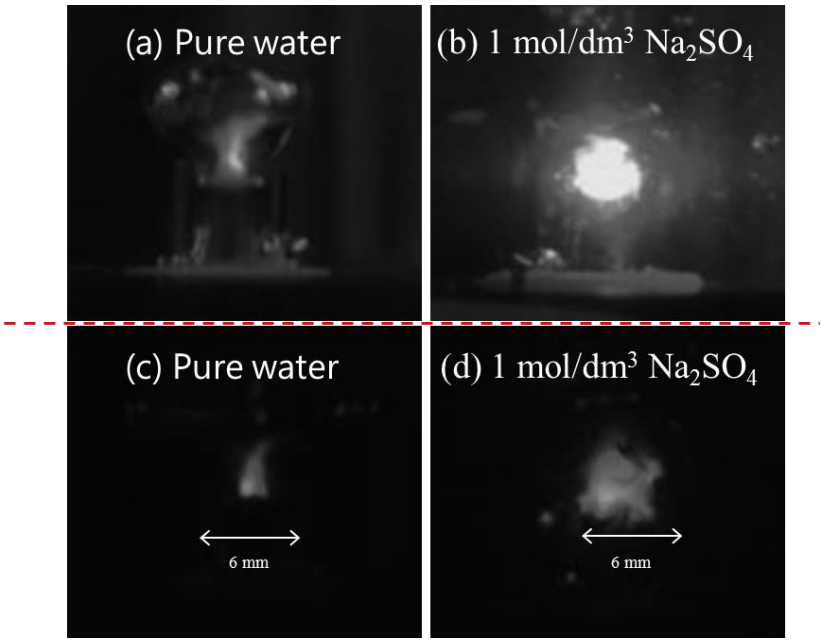

Fig. 3-6. Image of RF plasma generated in (a), (c) pure water and (b), (d) 1 mol/dm^3 Na_2SO_4 obtained using a CCD camera. (a) and (b) were taken through a ND filter. (c) and (d) were taken through a H-alpha pass filter (FWHM = 35 nm and centered at 656 nm)

overestimation of the discharge size, photographs were taken through an H-alpha pass filter (Baader Planetarium, FWHM = 35 nm centered at 656 nm). The size of the plasma can be evaluated by comparing with a quartz glass tube (OD: 6 mm). The filtered photographs of plasmas in pure water and in 1.00 mol/dm^3 Na_2SO_4 solution are presented in Fig. 3-6(c) and (d), respectively, and show distinct plasma sizes. In pure water, plasma with a width of 2.1 mm and a height of 3.0 mm was formed on the surface of the electrode. In Na_2SO_4 solution at 1.00 mol/dm^3, the plasma was 4.3 mm in width and 4.3 mm in height. With an increase in the Na_2SO_4 concentration, the size of the plasma increased. We postulate that the electric field causes the Na^+ and SO_4^{2-} from the Na_2SO_4 solution to collide with the copper electrode to generate greater electron emission and thus facilitate plasma generation. As shown in Fig. 3-4(b), the percentages of the generated gas of CO, CO_2 and CH_4 increased with concentration of Na_2SO_4. This suggests that cellulose decomposition was promoted by expansion of the discharge region and stability of discharge.

To estimate the gas temperature of the plasma, we measured the spectral lines of •OH between 306 and 320 nm and compared them with the calculated values. This is because the lines of •OH strongly depend on rotational and vibrational temperatures and has often employed to estimate temperature when plasma contains water molecules [68]. Fig. 3-7 shows the measured spectral lines for the plasma with Na_2SO_4 concentrations of 0.01 mol/dm^3, 0.10 mol/dm^3, and 1.00 mol/dm^3. The calculated spectrum for 3500 K and 4500 K are shown in Fig. 3-7(e ~ f). In this calculation, LIFBASE code was used [84]. In order to compare these lines with calculated ones, we introduce a fitting parameter,

$$\delta_T^2 = \left(\frac{f_1}{f_3} - \frac{g_1(T)}{g_3(T)}\right)^2 + \left(\frac{f_2}{f_3} - \frac{g_2(T)}{g_3(T)}\right)^2$$

where f_1, f_2, f_3 and g_1(T), g_2(T), g_3(T) correspond to the peaks of the measured and calculated spectral lines of 306.4 nm, 306.8 nm and 309.0 nm, respectively. Although the rotational temperature T_{rot} and the vibrational temperature T_{vib} can be set to be different in the LIFBASE code, we perform calculation here under the condition of T_{rot} = T_{vib} = T. This is because different values of these

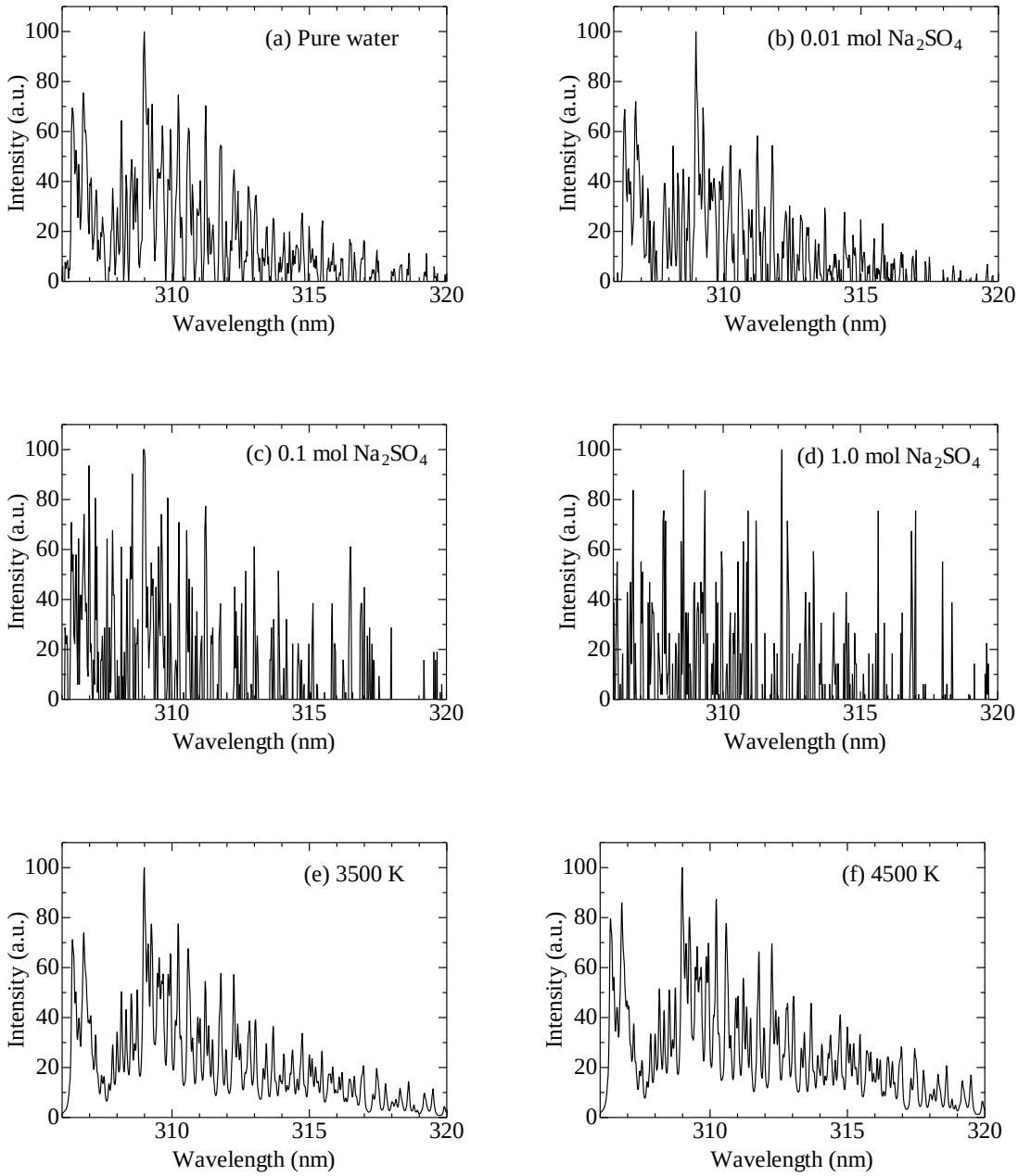

Fig. 3-7. Spectral lines of •OH in (a) pure water, (b) 0.01 mol/dm^3 Na_2SO_4, (c) 0.10 mol/dm^3 Na_2SO_4, and (d) 1 mol/dm^3 Na_2SO_4. (e) and (f) Spectral lines corresponding to calculated spectra at 3500 K and 4500 K.

temperatures cannot reduce the parameter δ_T^2. When the solution are pure water and 0.01 mol/dm^3 Na_2SO_4, δ_T^2 become minimum at 3500 K. This suggests that the plasma temperature does not strongly depend on Na_2SO_4 concentration. However, when the solution are 0.10 mol/dm^3 Na_2SO_4 and 0.01 mol/dm^3 Na_2SO_4, δ_T^2 cannot be sufficiently small. We suspect that in the case of using 0.10 mol/dm^3 and 1.00 mol/dm^3 Na_2SO_4, sufficient emission intensity for fitting did not be obtained.

3- 3 - 3 Production amount of H_2O_2

•OH has a strong oxidizing power that can decompose organic matter. The amount of OH radicals generated is an important parameter in the organic matter decomposition by plasma. H_2O_2 is produced by the generation of RF plasma in water [85]. More specifically, H_2O_2 is produced in the bubbles surrounding the plasma or in the immediate aqueous environment around the bubbles by the following recombination process [86]:

$$2OH\cdot \rightarrow H_2O_2.$$

Therefore, the H_2O_2 production amount correlates with the •OH production amount.

After the solutions were exposed to the RF plasma for 8 min, H_2O_2 concentration was determined colormetrically in which 4-aminoantipyrine was acted upon by an enzyme to change colors (DPM-H_2O_2, Kyoritsu Chemical-Check Lab). The concentration of H_2O_2 versus Na_2SO_4 concentration is shown in Fig. 3-8. H_2O_2 concentration in the cellulose suspensions was less than the H_2O_2 concentration in pure water due to the consumption of •OH for decomposing cellulose. Even though the production gas increased, the concentration of H_2O_2 decreased with Na_2SO_4 concentration. It has been found that copper electrode damage is significant when the concentration of Na_2SO_4 is high. It is considered that the OH radical reacts with these copper or hydrogen peroxide reacts with the copper ion. However, the clear reaction path is unknown and it is a future task.

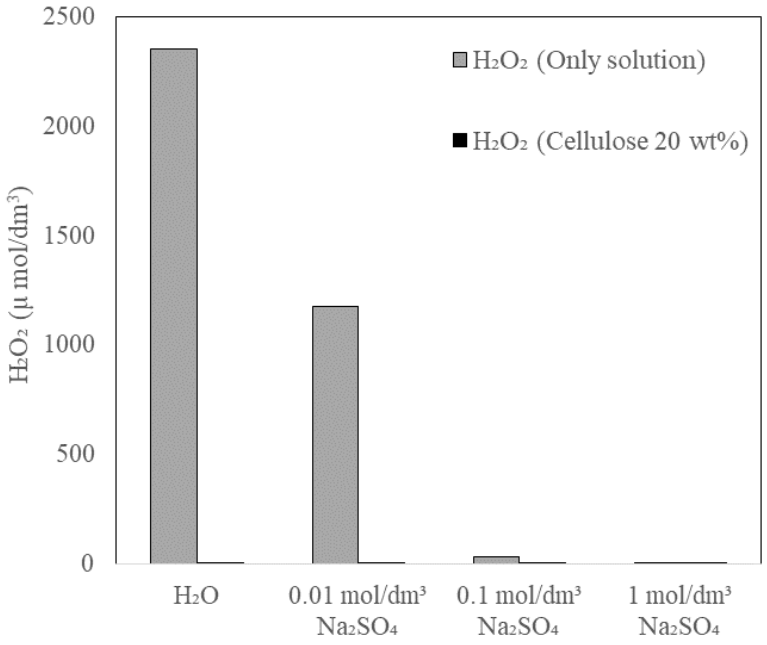

Fig. 3-8. Average intensity of ˙OH line, I_{OH}, (orange) versus Na_2SO_4 concentration. The blue and gray bars denote the concentration of H_2O_2.

3- 3 - 4 Water soluble organic substance

Fig. 3-9. shows the total ion chromatograms of the supernatant solutions after the experiment. It was inferred that the compound of the peak at 26.6 retention time was elution from the column because its mass spectrum was a compound of silica. Organic substances were not detected in the GC–MS. Since all of the cellulose is gasified in the high reaction field of the plasma, water-soluble organic substances is not produced.

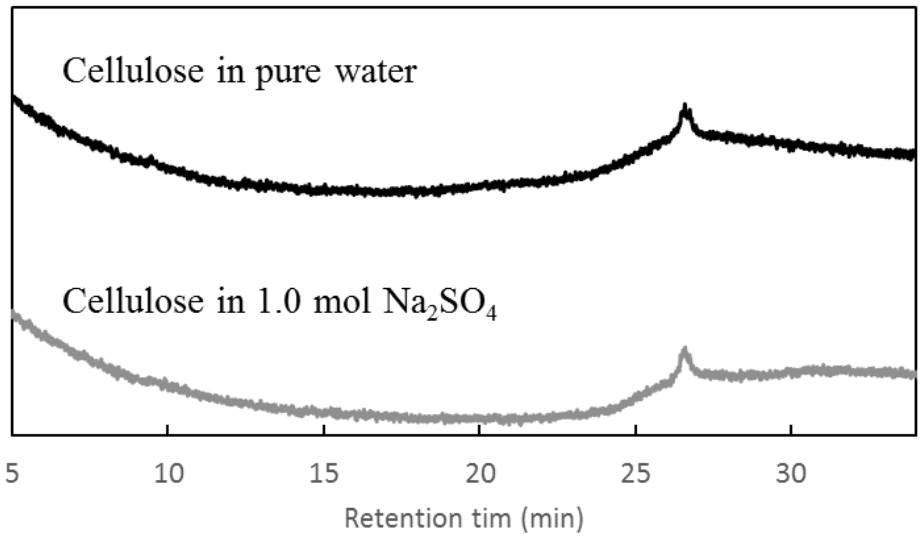

Fig. 3-9. Total ion chromatograms of the supernatant solutions after the experiment.

3 – 4 Conclusion

Decomposition of cellulose suspensions in 0.01 to 1.00 mol/dm^3 Na_2SO_4 and pure water was done using 27.12-MHz in-liquid plasma, and the production rates of gas products were also measured. Components of the product gas in the decomposition of cellulose by plasma were O_2, H_2, CO, CO_2, and CH_4, and the proportion of H_2 was about 60 to 70%. Na_2SO_4 increased the gasification efficiency of the solutions and the plasma size increased with Na_2SO_4 concentration. The gas temperature of plasma was approximately 3500 K in both pure water and 0.01 mol/dm^3 Na_2SO_4. The production of H_2O_2 decreased with Na_2SO_4 concentrations. Detection of H_2O_2 generation was minimal in cellulose suspensions. Organic substances were not detected in the supernatant solutions after the experiment.

Chapter 4. Production of hydrogen and monomer aromatics by in-liquid plasma treatment of lignin

4 – 1 Introduction

The present chemical industry relies on fossil fuels. Phenolic compounds and aromatic hydrocarbons (BTX) such as benzene and toluene play an important role as raw materials for the production of basic chemical products. Lignin is one of the main constituents of wood (18−40 wt%) [87]. Lignin has a large number of benzene rings and has drawn great interest as a new raw material for the production of aromatic monomers [88]. There are many proposed methods to decompose lignin, such as thermal decomposition and supercritical fluid extraction [89–93].

Hydrogen energy is the most promising energy source to enable sustainable development. Many scientists are working on improving the current H_2 generation methods [73,74,78]. Previous studies have described the decomposition of solutions, such as water, waste oil, and cellulose suspensions for H_2 production, using in-liquid plasma [70,83,94]. Plasma is generated in the solutions by applying a radio frequency (RF) as well as microwave radiation [1,2]. Hydrogen production efficiency obtained using in-liquid plasma was 0.045 μmol/J to 0.259 μmol/J for the decomposition of a cellulose solution and 0.021 μmol/J for the decomposition of n-dodecane [10,83]. However, for practical applications, it is necessary to increase the hydrogen production efficiency or to generate other valuable byproducts.

The purpose of this study is to convert lignin solution in methanol into an aromatic monomer and hydrogen using in-liquid plasma, which generates a chemical reaction that reaches up to temperature of 3500 K [67,68].

4 – 2 Experimental material and methods

Methanol (100 mL) was used as the solvent for 0.1–5.0 g of lignin (catalogue number L0045 Tokyo Chemical Industry Co., Ltd.); a solution containing 99 mL methanol and 1 mL benzene was alternatively used as the solvent for comparison. Only the soluble part of the lignin, which represents about 60–70 % of the total lignin, was used by filtering the lignin solution through a filter paper (Advantec Quantitative Filter Paper No. 3.). Part of the filtrate was volatilized in a water bath and weight of the remaining lignin was determined to dilute the solution with methanol to reach the target concentration. A schematic of the apparatus used for the decomposition of lignin dissolved in methanol is shown in Fig. 4-1. A copper electrode with a diameter of 3.0 mm was inserted vertically from the bottom of the reactor and was enveloped by a ceramic tube, which is composed of a dielectric substance to minimize energy loss. An aluminum circular plate (diameter: 39 mm) with a tiny hole in the center was placed over the counter electrode. The gas production rate was measured and the produced gases were analyzed using gas chromatography. The solution was analyzed before and after the experiment by gas chromatography–

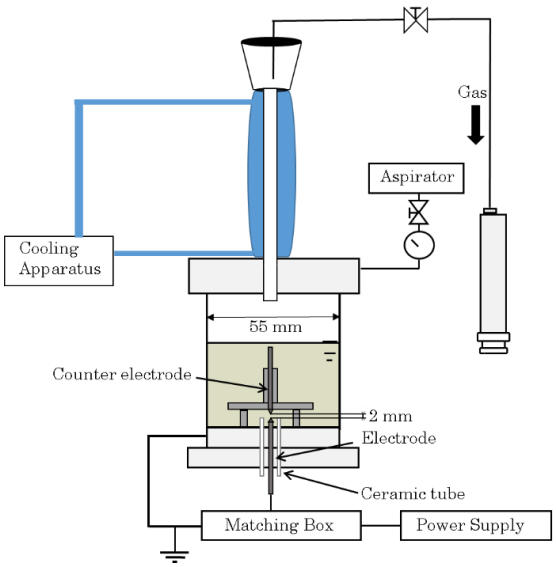

Fig. 4-1. Experimental set-up for the decomposition of lignin dissolved in methanol.

mass spectrometry.

The experimental procedures are as follows: the pressure of the reactor was first reduced to the range of 5–7.5 kPa using an aspirator. Under this condition, the power input from a 27.12 MHz radio frequency generator and the impedance were simultaneously adjusted using a matching box. Plasma was discharged at the tip of the electrode instantly after the electric breakdown. The discharge power was 200 W, which was calculated by subtracting the reflected power from the input power. The reactor valve was opened once the inner pressure of the reactor reached the atmospheric pressure. The produced gas was then sampled by an air-tight glass syringe.

The spectra of the plasma generated were obtained using an optical emission spectroscope (Hamamatsu PMA11) in the range of 200–950 nm. The light emitted from the plasma was guided to a spectrometer through a quartz window. The quartz window was 5 mm thick and it was mounted on the side of the reactor and fixed using an acrylic cap. The optical fiber was mounted in front of the quartz window.

A Shimadzu GC-8A instrument was used to analyze the produced gases. The column used was a SHIMADZU GC Stainless Column SHINCARBON ST (length, 4 m; diameter, 3 mm). The temperature was controlled from 60 °C for 6.0 min to 160 °C at a rate of 10.0 °C/min and it was held at 160 °C for 14 min. An argon carrier gas was applied at a flow rate of 50 mL/min. The produced gases were identified based on their retention times compared with those of authentic gases.

Shimadzu GCMS-QP2010 Ultra and GC-2010 Plus instruments were used to analyze the solution. The capillary column was a Rxi-1 ms column (length, 30 m; diameter, 0.25 mm; thickness, 0.25 μm). The temperature was controlled from 40 °C for 1.0 min to 300 °C at a rate of 10.0 °C/min and it was held at 300 °C for 10 min. A helium carrier gas was applied at a flow rate of 1.5 mL/min. The injector temperature was 230 °C. One microliter of the solution was directly injected. The lignin-derived monomeric products were identified from their mass spectra by comparing their retention times with those of authentic compounds.

4 – 3 Results and discussion

4- 3 - 1 Gas productions rate and gas composition

Fig. 4-2 shows the gas production rate. The product gas was composed of H_2, CO, CH_4, C_2H_2, CO_2,

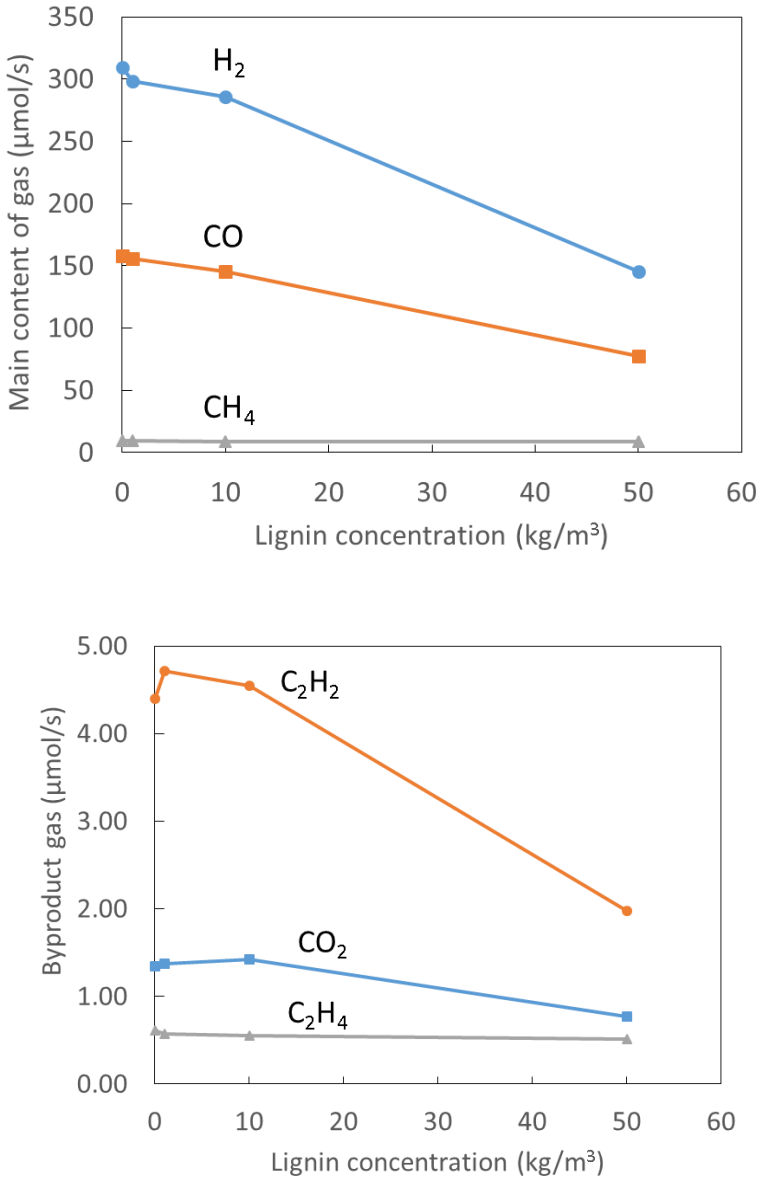

Fig. 4-2. Gas production rate as a function of the lignin concentration.

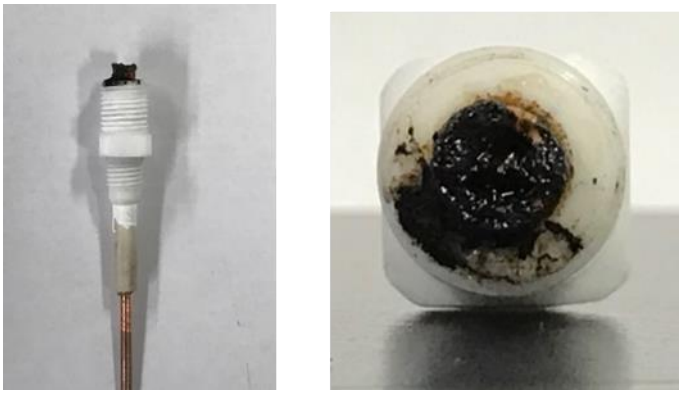

Fig. 4-3. Pictures of the periphery of the electrode after the experiment when using a lignin solution with a concentration of 10 kg/m^3.

and C_2H_4. The gas production rates with lignin solutions of concentrations between 1 and 10 kg/m^3 were slightly lower than those with a plain methanol solution. It is considered that gasification of lignin occurs near the center of the plasma. However, since it is difficult for nonvolatile polymeric lignin to exist in a plasma state, it is only slightly gasified. The energy of the plasma is used to generate the aromatic compounds, and the gas production rate decreases along with the concentration of lignin. In the 50 kg/m^3 condition, the plasma was unstable and disappeared after 2.5 min of plasma irradiation. The pictures of the periphery of the electrode after the experiment when using a lignin solution with a concentration of 10 kg/m^3 are shown in the Fig. 4-3. After the experiment, lignin was deposited near the electrode, and the glass tube covering the electrode was partially melted. It was concluded that lignin accumulated on the electrode or between the electrode and the ceramic tube at this point could not be decomposed, impeding plasma generation.

4- 3 - 2 Qualification and quantification of by-products

The results of the GC–MS analysis revealed some products, including benzene, toluene, and phenol. The quantity of each of these products was also determined. Fig. 4-4 shows the amounts of benzene, toluene, and phenol produced as a function of the plasma processing time with a lignin concentration of

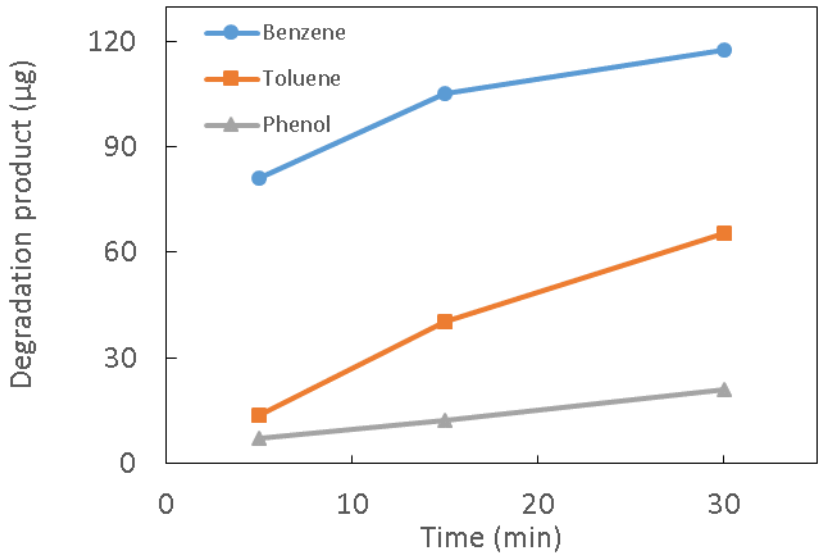

Fig. 4-4. Amounts of benzene, toluene, and phenol produced as a function of the plasma processing time (lignin 1 kg/m^3).

Table. 4-1. Amounts of the components produced.

solute (g)	pretreatment volume (mL)	plasma processing time (min)	obtained benzen (μg)	obtained toluene (μg)	obtained phenol (μg)
lignin 0.1 g	100	15	105	40	12
benzen 0.88g	100	15	–	517	59

1 kg/m^3 of solution. These results show that benzene was produced at a much quicker rate compared with toluene or phenol.

A mixed solution containing 99 mL methanol and 1 mL benzene was used for comparison. Table 4-1 shows a comparison of the amounts of the various components produced for the lignin solution and the benzene solution. Toluene and phenol were identified in both solutions after plasma treatment.

4- 3 - 3 Plasma emission analysis and reaction mechanism

Optical emission spectroscopy was used to characterize the plasma [57,62]. Fig. 4-5 shows the spectra of methanol solution at 100 kPa. At 100 kPa, the aspirator was stopped and the container was opened to the atmosphere. Emission lines from atomic hydrogen, including H_α (656 nm) and H_β (486 nm), OH (306 nm), CH (431 nm), and C_2 (460–480 nm and 500–515 nm), were observed and CO emission peaks were observed in the range of 250–650 nm. The methyl radical (CH_3) could not be observed because of the limited wavelength range of the optical measurement. However, the emission lines of OH and CH observed with methanol suggests that production of CH_3 as follows:

OH radicals and CH_3 radicals are produced in the plasma by the decomposition of methanol molecules:

$$CH_3OH \rightarrow CH_3\cdot + OH\cdot \quad (1)$$

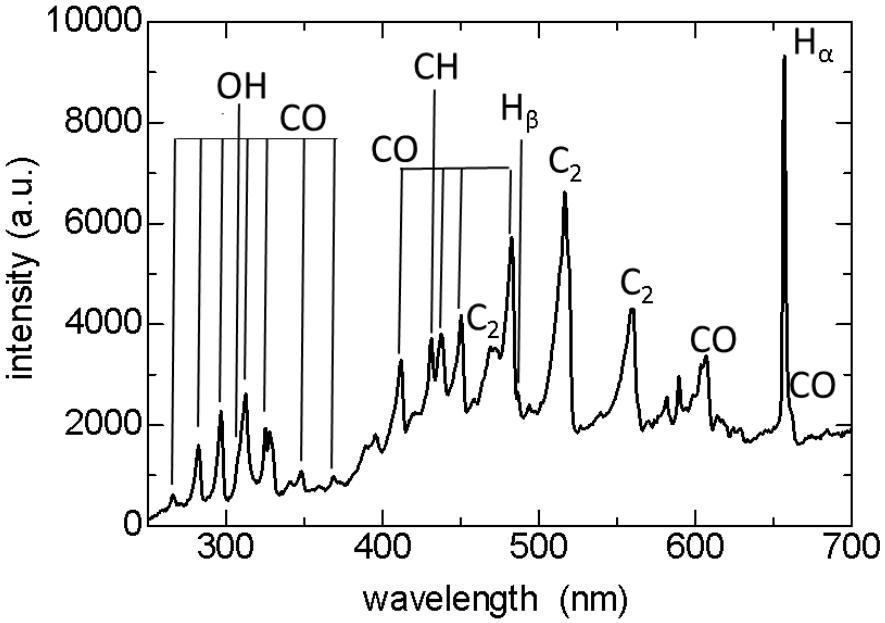

Fig. 4-5. Emission spectrum of plasma generated in methanol.

Then, CH_2 and CH radicals were produced as a result of successive activation processes of CH_3:

$$CH_3\cdot \rightarrow CH_2\cdot \rightarrow CH\cdot \quad (2)$$

Benzene, toluene, and phenol were produced by the following processes. First, the bonds around the benzene ring of lignin were broken in the plasma. Then, the OH radicals and CH_3 radicals reacted with benzene:

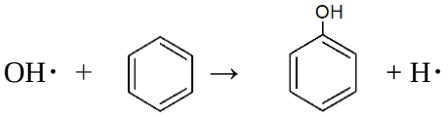

(3)

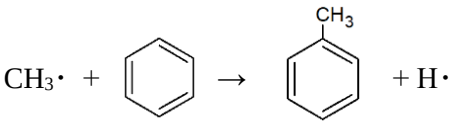

(4)

A significant amount of research regarding the production of phenol by a reaction of the generated OH radicals with benzene has been reported [95,96]. Some amount of the produced benzene gets converted into radicals owing to their collision with electrons:

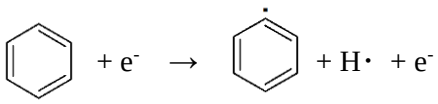

(5)

Toluene and phenol are produced easily via a recombination reaction of these radicals:

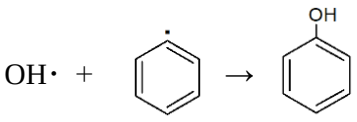

(6)

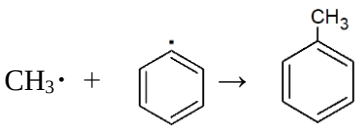

(7)

In Fig. 4-4, the reason why benzene was produced at much quicker rate compared to toluene or phenol is considered as follows:

Benzene is produced by decomposition of the lignin solution. Subsequently, the methyl radical and the OH radical generated by the cleavage of methanol react with benzene to produce toluene and phenol. However, not all benzene reacts with radicals. It is considered that since the production rate of benzene is greater than the amount of its reacting with radicals, the amount of benzene production is larger than that of toluene and phenol production.

The amounts of benzene, toluene, and phenol produced for various lignin concentrations are shown in Fig. 4-6. The amounts of these products increased with the concentration of lignin. In particular, the amount of phenol produced increased significantly as the lignin concentration increased. The ratio of toluene to phenol produced by the decomposition of the benzene solution was approximately 8.8, as shown in Table 4-1. However, the ratios of toluene to phenol produced by the decomposition of the lignin solution were approximately 2.0 with 1 kg/m^3 of lignin, 0.36 with 10 kg/m^3 of lignin, and 0.08

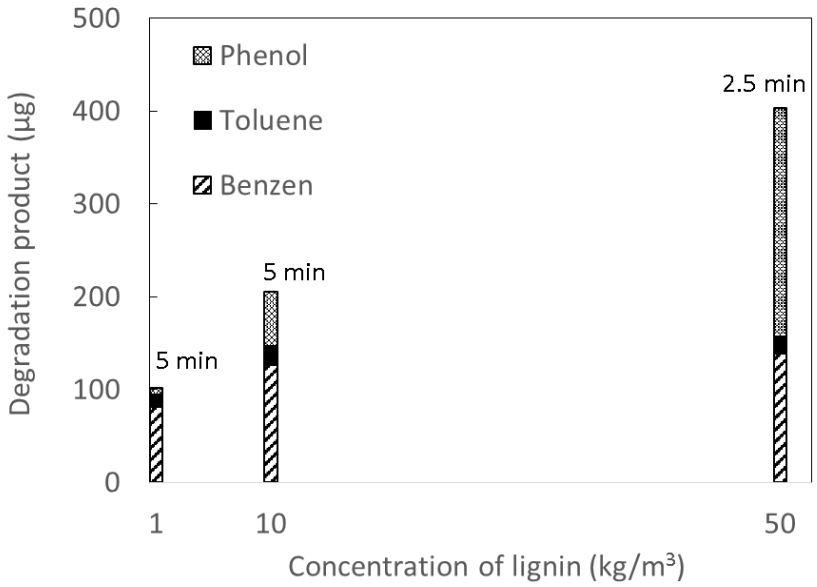

Fig. 4-6. Amounts of benzene, toluene, and phenol produced with various lignin concentrations.

with 50 kg/m^3 of lignin. This result suggests that the production of phenol from a lignin solution occurs not only via the reactions shown in Eqs. (3) and (6) but also occurs directly by the decomposition of lignin. The amount of the decomposition products increased with the concentration of lignin. However, most of the lignin decomposition did not advance to benzene so phenol was produced.

4 – 4 Conclusion

The decomposition of lignin in methanol was achieved using a 27.12 MHz RF in-liquid plasma treatment. The produced gas was composed of H_2, CO, CH_4, C_2H_2, CO_2, and C_2H_4. Benzene, toluene, and phenol were produced and the amounts of these products increased proportionally with the concentration of lignin. Atomic hydrogen, including H_α (656 nm) and H_β (486 nm), OH (306 nm), CH (431 nm), and C_2 (460–480 nm and 500–515 nm), were identified based on the emission spectrum; CO emission peaks were observed in the range of 250–650 nm. The ratio of toluene to phenol produced by the decomposition of the benzene solution was approximately 8.8, while those produced by the decomposition of solutions containing 1, 10, and 50 kg/m^3 of lignin were 2.0, 0.36, and 0.08, respectively.

Chapter 5. Formation of two kinds of carbon with different properties by acetone decomposition using in-liquid plasma method

5 – 1 Introduction

Industrial waste solvents are discarded by various factories and research institutions. The main chemical components of such waste solvent are volatile organic compounds (VOC), such as acetone, toluene, and methanol. VOCs are the primary cause of photochemical oxidants and suspended particulate matter; therefore, facilities that emit VOCs have been regulated [97]. Researchers are interested in the problem caused by the high toxicity of VOC and the air pollution level of some cities which is considered to be caused by VOC was measured [98,99]. Most waste solvent treatment methods involve combustion. However, such methods emit CO_2, which is considered a causative substance of global warming. In addition, such methods incur significant energy costs.

Various methods to reduce VOC emissions, such as biodegradation, combustion, adsorption, and plasma decomposition, have been proposed [100–103]. The VOC concentration that can be treated by each method differs; however, in most cases these methods treat gaseous VOC. In addition, various methods to decompose VOC using plasma under a wide range of gas flow velocities and VOC concentrations have been reported to date. Non-thermal plasma processes (NTPs) such as dielectric barrier discharges (DBD) [104] and corona discharges [105] have been used for the decomposition VOC at a low concentration of several hundred to a 1000 ppm or so. However, the removal efficiency is low and it is not suitable for the treatment of high concentration VOCs [106]. For example, Chang and Lin (2005) reported the decomposition of VOCs (1100 ppm) by DBD with TiO_2 and glass pellets. The maximum removal efficiency was 80% and energy efficiencies was $1.3 \times 10^{-6}\,\mathrm{mol}J^{-1}$ at an operating flow rate of 36 L s^{-1} [107]. On the other hand, the use of thermal plasma for VOC

decomposition can achieve high concentration of VOC decomposition and high removal efficiency due to high temperature and high reactivity [108]. Narengerile et al. (2012) reported that 5 mol% acetone was decomposed by water plasmas with removal efficiency of 99.8% and energy efficiencies of 1.7×10^{-7} molJ^{-1} at an acetone solution feed rate of approximately 72 mg s^{-1} [109]. However, high power consumption and damage to electrodes prevent the practical use.

Hydrogen energy is considered the most promising source of energy to enable sustainable development. Many scientists are working on improving existing H_2 generation methods [73,74,79]. Previous studies have described the decomposition of solutions, such as water, hydrocarbon, and cellulose suspensions, for H_2 production using in-liquid plasma, which generates a high temperature chemical reaction field [10,12,83,94]. Recently, Shiraishi. R. et al. reported that the hydrogen production efficiency reached 0.37 Nm^3/kWh in methanol decomposition combining in-liquid plasma and metal catalyst [11]. Plasma is generated in the solutions by applying radio frequency or microwave radiation [1,2]. With this method direct decomposition of harmful substances is possible without requiring a catalyst. In particular, when applied to the decomposition of organic matter, this method, which generates solid carbon, has been very effective in suppressing the amount of CO_2 produced. By using in-liquid plasma, hydrogen energy and valuable materials may be produced from waste solvent.

Acetone is a VOC that is widely used as an organic solvent. In this study, acetone was used as a model waste solvent and was decomposed using an in-liquid plasma method at atmospheric pressure. Here, the purpose was to convert acetone into hydrogen and other valuable substances while suppressing the generation of CO_2.

5 – 2 Material and methods

A schematic of the apparatus used for the decomposition of acetone and the photograph of the plasma discharge are shown in Fig. 5-1. A tungsten electrode with a diameter of 1.5 mm was inserted vertically

from the bottom of the reactor and was enveloped by a glass tube, which is composed of a dielectric substance to minimize energy loss.

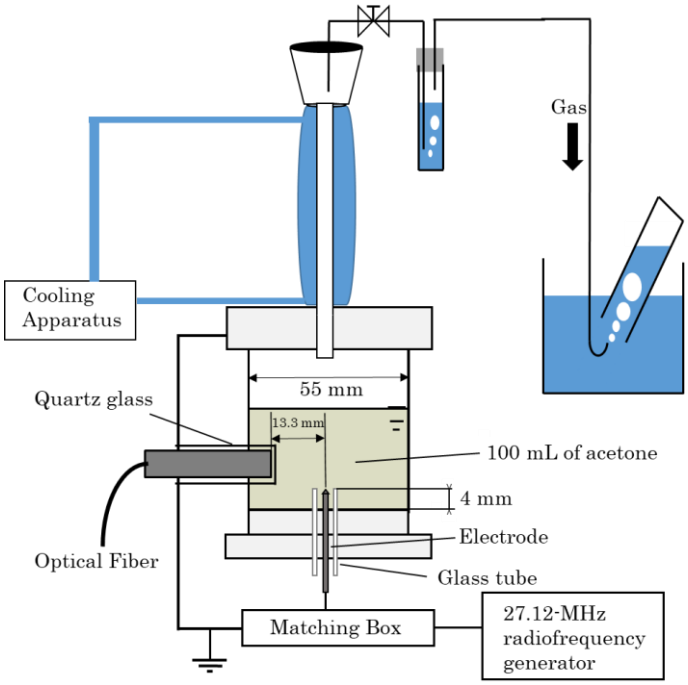

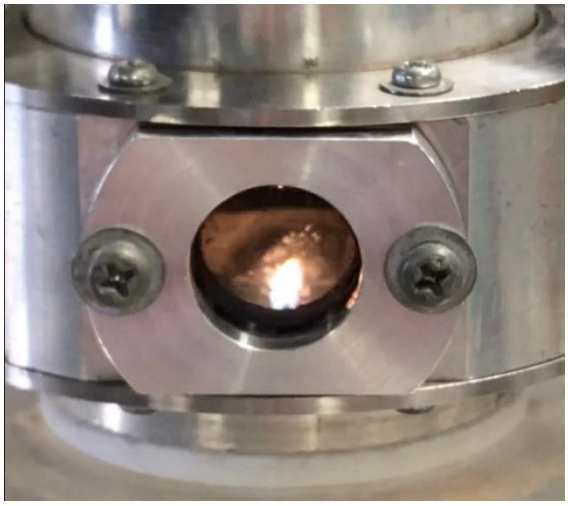

Fig. 5-1. Apparatus used to decompose acetone and the photograph of the plasma discharge.

The experiment proceeded as follows. Under atmospheric pressure conditions, the power input from a 27.12 MHz radio frequency generator and the impedance were adjusted simultaneously using a matching box. Plasma was discharged at the tip of the electrode immediately after the electric breakdown. The discharge powers, which were calculated by subtracting the reflected power from the input power, ranged from 308 to 417 W. The gas produced by the decomposition of acetone was cooled using a Liebig condenser at 0 ℃ and then through 30 mL of acetone. The produced gas was collected in water. The irradiation time of plasma was 4 minutes in all experiments. After plasma irradiation, the solution was filtered using with 0.1 μm filter paper (Omnipore Membrane Filters), and the solids on the filter paper and the filtered solution were collected.

A Shimadzu GC-8A instrument equipped with TCD detector was used to analyze the produced gases. A SHIMADZU GC Stainless Column SHINCARBON ST (length, 4 m; diameter, 3 mm) was used. The temperature was controlled from 60 °C for 6.0 min to 160 °C at a rate of 10.0 °C/min and it was held at 160 °C for 14 min. An argon carrier gas was applied at a flow rate of 50 mL/min. The produced gases were identified based on their retention times compared with those of authenticated gases.

A Shimadzu GC-8A instrument equipped with TCD detector was used to analyze the produced gases. A SHIMADZU GC Stainless Column SHINCARBON ST (length, 4 m; diameter, 3 mm) was used. The temperature was controlled from 60 °C for 6.0 min to 160 °C at a rate of 10.0 °C/min and it was held at 160 °C for 14 min. An argon carrier gas was applied at a flow rate of 50 mL/min. The produced gases were identified based on their retention times compared with those of authenticated gases.

A Shimadzu GCMS-QP2010 Ultra and GC-2010 Plus instruments were used to analyze the filtered solution and the acetone solution that trapped the produced gas. The capillary column was a DB-FFAP column (length, 30 m; diameter, 0.25 mm; thickness, 0.50 μm). The temperature was controlled from 40 ℃ for 1.0 min to 250 °C at a rate of 10.0 °C/min and held at 250 °C for 10 min. A helium carrier gas was applied at a flow rate of 1.5 mL/min. The injector temperature was 230 °C. One microliter of the solution was injected directly.

A photonic multichannel analyzer (PMA-11, HAMAMATSU) was used to measure plasma emissions spectroscopically. The measured spectrum ranged from 200 to 950 nm. Light from the plasma was

guided to the spectroscope through quartz glass. The quartz glass was welded to the hollow glass and fixed to the side of the electrode, and the optical fiber was mounted in front of the quartz window.

To quantify the degree of acetone decomposition and to evaluate the proposed method, the decomposition amount and energy efficiency were calculated as follows:

$$\text{Decomposition amount } [mol] = \frac{H_g[mol]}{H_a}$$

$$\text{Energy efficiency } [molJ^{-1}] = \frac{Decomposition\ amount\ [mol]}{Required\ discharge\ energy\ [J]}$$

where H_g is the number of total hydrogen atom mole in the product gas and H_a is the number of hydrogen atoms in the acetone molecule.

5 – 3 Results and discussion

5- 3 - 1 Gas productions rate and gas composition

The gas production rate at each discharge power is shown in Fig. 5-2. The gas production rate tended to be larger at higher discharge power. As the discharge power increases, the temperature of acetone in the vicinity of the tip of the electrode increases, making it easier to generate bubbles. Plasma is generated in bubbles, so it is considered that the higher discharge power stabilizes the plasm for a long time and the decomposition amount of acetone increases. It is also considered that high discharge power increases the plasma volume.

The composition of the produced gas at each discharge power is shown in Fig. 5-3. The produced gases were H_2, CO, CH_4, C_2H_2, C_2H_4, C_2H_6, and CO_2. About 70% of the produced gas was composed of H_2 and CO and can be used as synthesis gas. The composition of the produced gasses remained largely

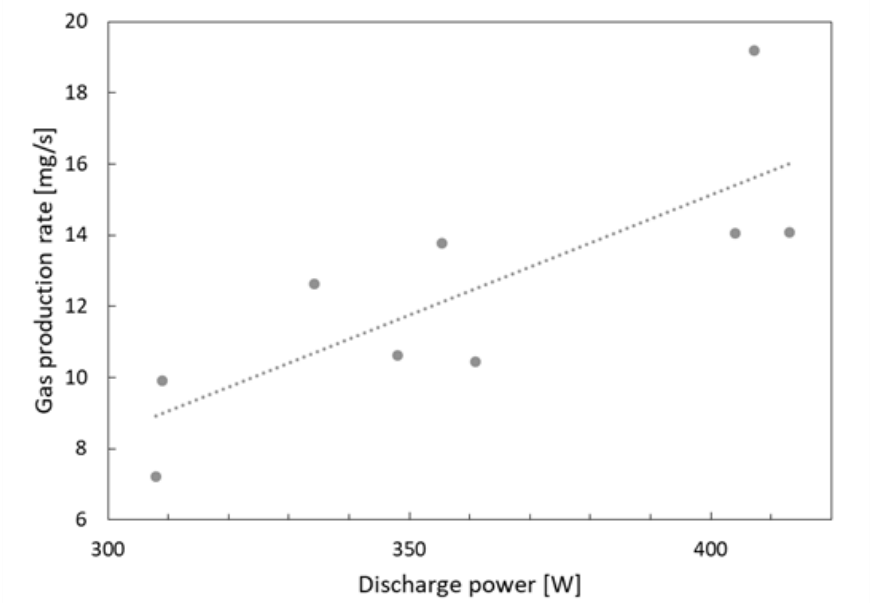

Fig. 5-2. Gas production rate at different discharge power.

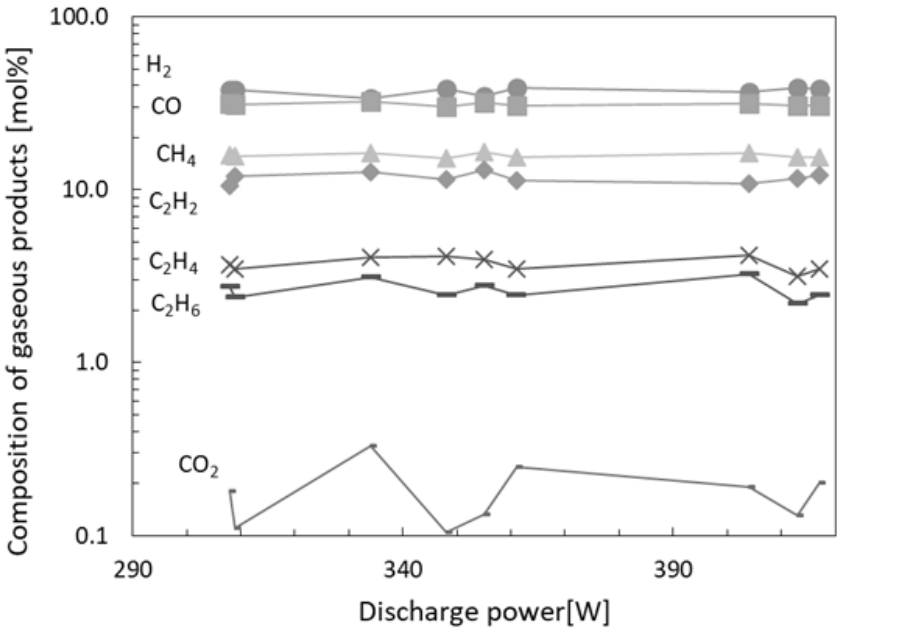

Fig. 5-3. Composition of produced gas at each discharge power.

unchanged regardless of changes in the discharge power. This indicates that the equilibrium state of the plasma does not change even if the discharge power increases. The maximum proportion of CO_2 in the produced gas was 0.25%. Up to more than 10% of CO_2 was discharged by the water plasma method where the atmospheric pressure conditions were the same as those employed in this study [109].

5- 3 - 2 Analysis of produced solid

Fig. 5-4 shows photographs of the acetone solution and lower part of the reactor before and after plasma irradiation and the obtained solids. A solid was produced by acetone decomposition and dispersed in the solution, which became black. Two types of solids with different appearances were obtained by decomposing the acetone solution. One was a powdery solid obtained by filtering the solution. The other was a stick solid extending from the electrode. Note that the selectivity of the powder and solid solids was a ratio of approximately 6:4 regardless of input power.

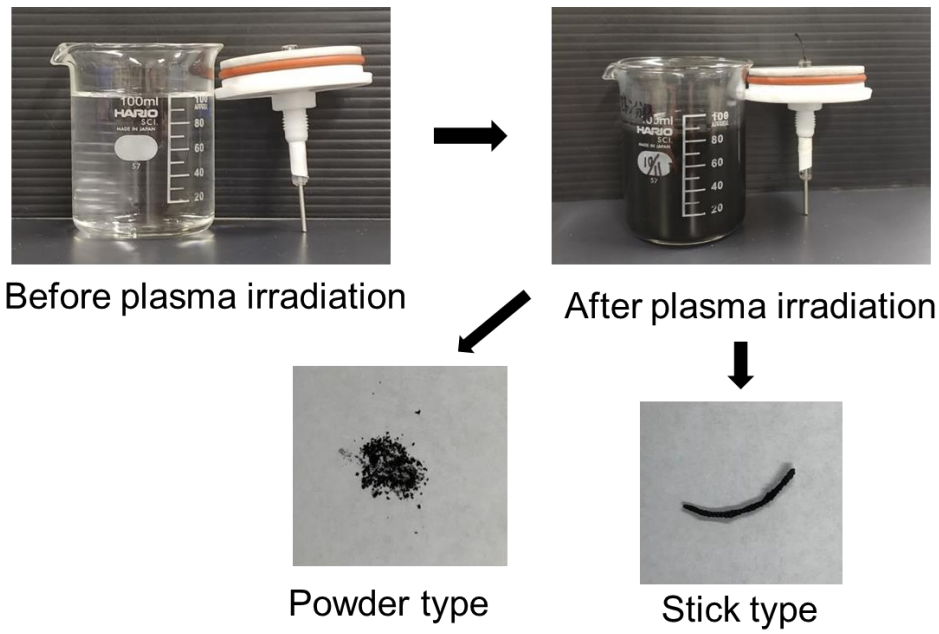

Fig. 5-4. Photographs of acetone solution, lower part of the reactor before and after plasma irradiation, and the obtained solids at the discharge power of 348 W.

The solid production rate at each discharge power is shown in Fig. 5-5. The solid production rate was calculated by measuring the combined weight of the powder and stick solids. The solid production rate tended to greater larger at higher discharge because the amount of acetone decomposition was enhanced with increasing discharge power. The weight of the tungsten electrode before and after plasma irradiation was measured. The weight reduction of the tungsten electrode was less than 0.1 mg with plasma irradiation for 4 minutes. Therefore, it is considered that there is no influence of tungsten particles in analysis of the produced solid.

The two types of solids were analyzed using an elemental analyzer and Raman spectrometry. The elemental analysis results revealed that the power type contained 94.9 wt% carbon, 1.6 wt% hydrogen, and 3.5 wt% oxygen. The stick type contained 98.2 wt% carbon, 0.7 wt% hydrogen, and 1.1 wt% oxygen.

The Raman spectrometry results are shown in Fig. 5-6. In the Raman spectra, the D-, G-, and 2D-bands appeared at approximately 1350, 1590, and 2700 cm^{-1} in both types solids. However, the peak shape differed. The D-band is caused by structure disorder and defect, whereas the G band is a

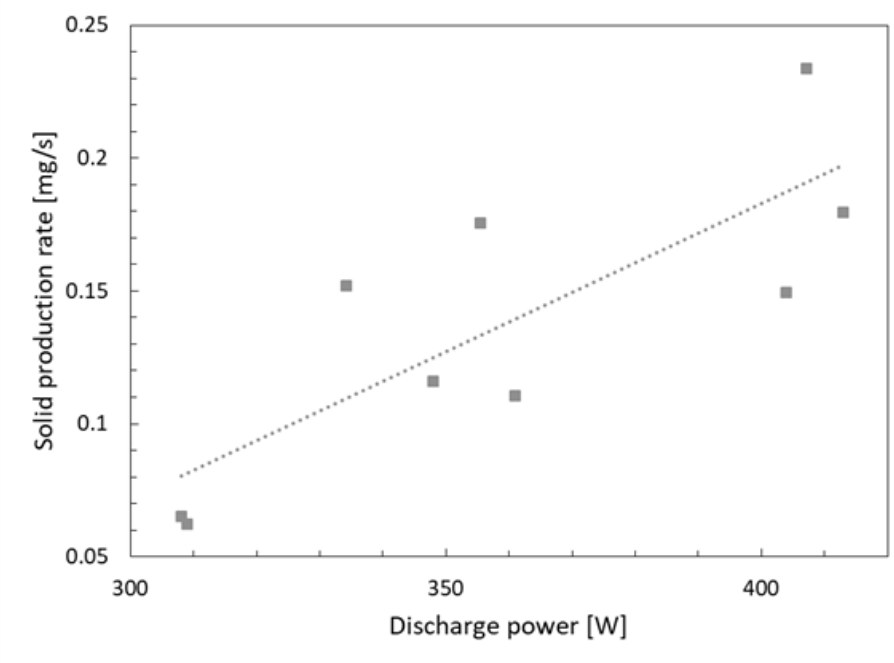

Fig. 5-5. Solid production rate at each discharge power.

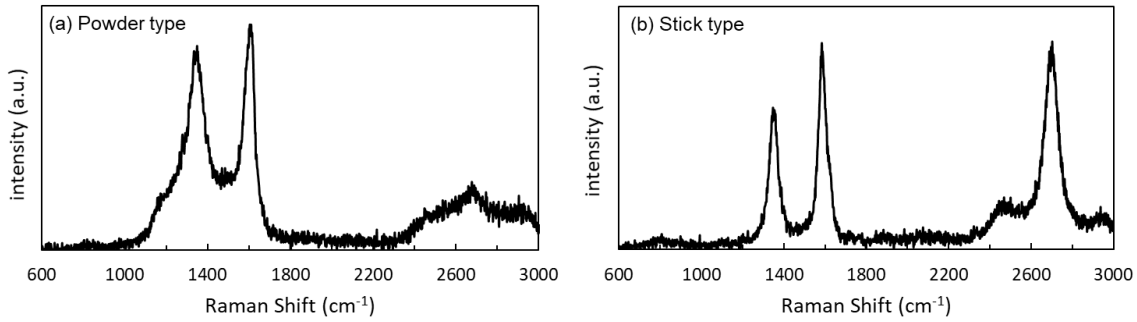

Fig. 5-6. Raman spectra of the two solids obtained from acetone decomposition.

characteristic peak of graphene that is derived from in-plane movement of carbon atoms. The ratio between the intensities of the D- and G-bands (I(D)/I(G)) is a crystallinity index for graphite because I(D)/I(G) = 0 for single-crystalline graphite [110]. The I(D)/I(G) ratio of the powder type was 0.90, whereas that for the stick type was 0.63. Therefore, the stick type is superior relative to crystallization. The 2D band showed strong frequency dependence on the excitation laser due to the double resonance process relating the phonon wave vector to the electronic band structure [111]. Single-layer graphene can be fitted with a single Lorentzian, but it consists of the sum of multiple peaks when it has two or more layers. Therefore, it is considered that the stick type is composed of graphene with the number of layers thinner than the powder shape.

Acetone in the plasma state has low density, rises in the bubble. Near the electrode tip, the electric field is most concentrated and the carbonization rate is high. As a result, acetone in the plasma state comes into contact the generated carbon before it is separated into the liquid; thus, the carbon is considered to grow upward from the bottom. These acetone are exposed to high temperature fields for a long period, and highly crystalline carbon is produced. As the distance from the electrode tip is increased, the plasma temperature is reduced, and the generated carbon is immediately dispersed in the liquid. As a result, the carbon crystallinity is considered to be low.

5- 3 - 3 Analysis of substances trapped in acetone and filtered solution

The acetone solution that trapped the produced gas and the filtered solution were analyzed by GCMS. The total ion chromatogram of the acetone solution that trapped the produced gas is shown in Fig. 5-7 (a), where the numbers represent the substances listed in Table 5-1 (a). It was found that eight types of

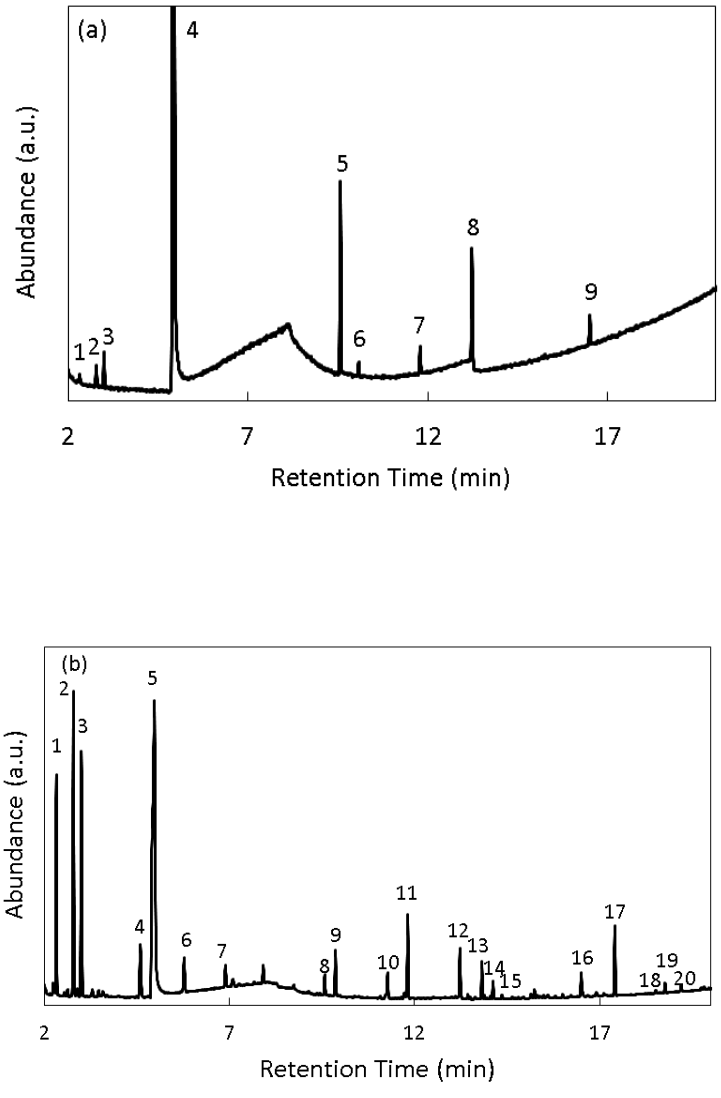

Fig. 5-7. Total ion chromatogram of (a) the acetone solution that trapped produced gas and (b) the filtered solution

organic matters were discharged, with the exception of acetone. However, water and diacetone alcohol were also slightly contained in the original acetone reagent. These organic matters have adverse effects on both the human body and the environment. In this method, a recovery system is required for such substances. The total ion chromatogram of the filtered solution is shown in Fig. 5-7 (b), where the numbers represent the substances listed in Table 5-1 (b). Although some peaks could not be identified as of this moment, twenty types of organic matters were identified, many of which were aromatic compounds. Among these organic matters, substances with relatively high molecular weight are not discharged to the outside, and are considered to be decomposed again by plasma.

Table. 5-1. Structural formula of (a) substance trapped in acetone solution and (b) substance contained in filtrate solution

(a)

No.	Product	Structure
1)	2-butanone	
2)	Benzene	
3)	Diacetylene	
4)	Water	
5)	Acetic anhydride	
6)	Diketene	
7)	Diacetone alcohol	
8)	Acetic acid	
9)	Triacetyl methane	

(b)

No.	Product	Structure
1)	2-butanone	
2)	Benzene	
3)	1,3-Butadiene	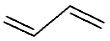
4)	Toluene	
5)	Water	
6)	Hepta-4,6-diyn-2-ol	
7)	Ethylbenzene	
8)	Acetic anhydride	
9)	Styrene	
10)	Hexa-1,3,5-triyne	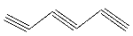
11)	Phenylethyne	
12)	Acetic acid	
13)	Methylphenylacetylene	
14)	Indene	
15)	2,5-Hexanedione	
16)	Triacetyl methane	
17)	Naphthalene	
18)	1,4-Diethynylbenzene	
19)	1-Methylnaphthalene	

20)	2-Methylnaphthalene	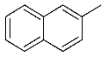

5- 3 - 4 Energy efficiencies of acetone decomposition

The energy efficiency of the acetone decomposition and hydrogen production are shown in Fig. 5-8. The energy efficiencies of the acetone decomposition and hydrogen production reached approximately

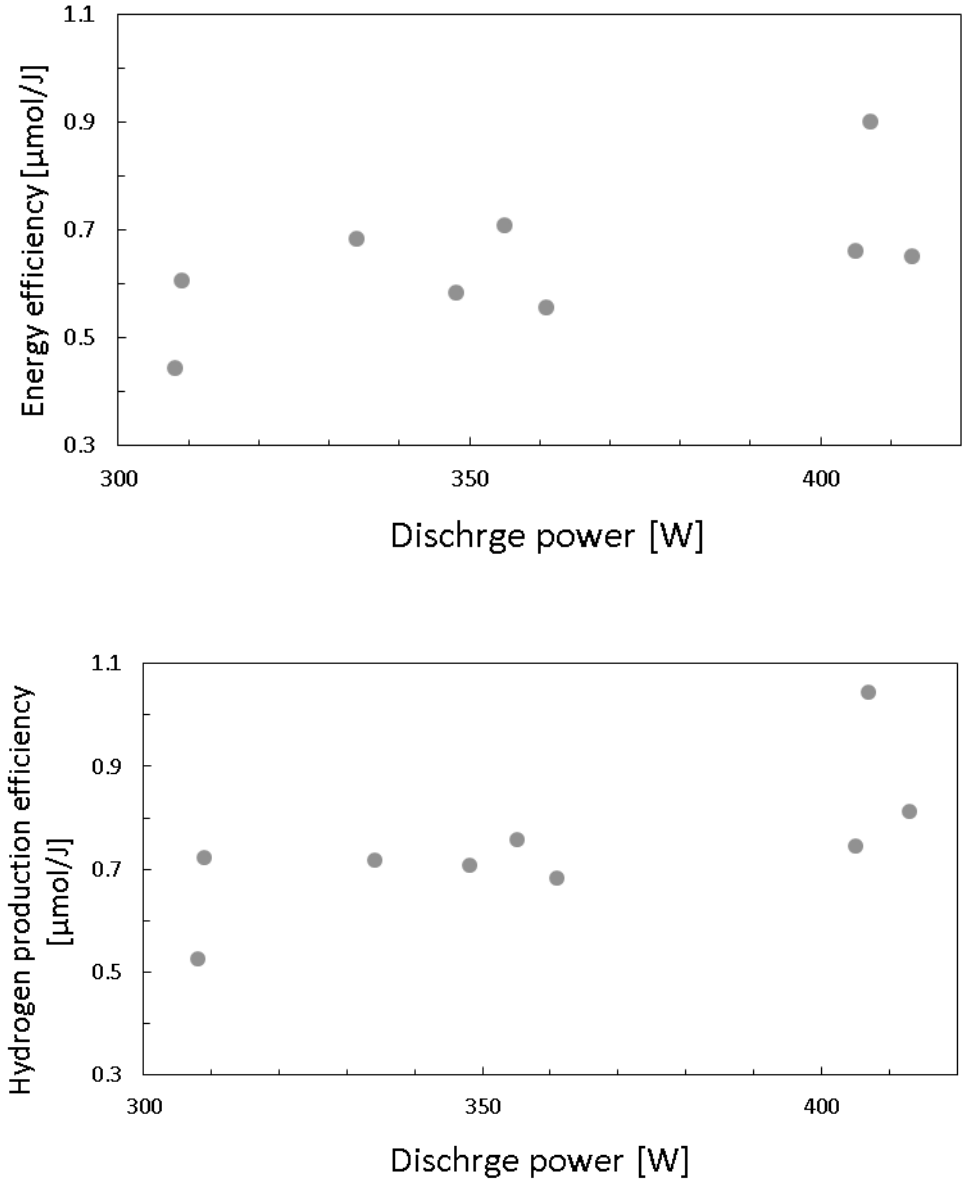

Fig. 5-8. Energy efficiency of (a) acetone decomposition and (b) hydrogen production at each discharge power

0.9 μmolJ^{-1} and 1.0 μmolJ^{-1} at a discharge power of 407 W. The energy efficiency of the acetone decomposition tended to be greater at higher discharge. In the decomposition of organic matter using the plasma of the previous research, decomposition efficiency tended to decrease as discharge power increased; however, but the opposite result was obtained. As the carbon grows from the electrode, the impedance changes. The impedance is adjusted by changing the resistance of the capacitor manually, and the plasma is generated; however, at low discharge power, there is a point at which the plasma becomes considerably unstable. Here, it is considered that this instability influences the decomposition efficiency of acetone.

5- 3 - 5 Spectroscopic measurement of plasma emission

The emission spectrum of the plasma is shown in Fig. 5-9. Here, excited species, such as CH (431 nm), C_2 (436 - 438 nm, 468 - 474, 510 - 517 and 547 - 564 nm), H_β (486 nm), Na (589 nm), H_α (656 nm), and O (777 nm and 845 nm) were confirmed. There was no change in the type of active species at any discharge power (308 to 413 W). Since Na is contained in the glass tube covering the electrode, it is considered that the light emission of Na is derived from the glass tube. Acetone absorbs the light of the plasma and nearly no light emission of the plasma of 230 to 330 nm can be confirmed. Therefore, multiple peaks could not be identified. Under the assumption that the plasma in the liquid is in thermal equilibrium, the intensity ratio of the Hα and H_β spectral lines is given by

$$\frac{I_{ij}}{I_{kl}} = \frac{\nu_{ij} A_{ij} g_i}{\nu_{kl} A_{kl} g_k} \exp\left(-\frac{E_i - E_k}{k T_{EX}}\right)$$

where T_{EX} is the excitation temperature, I_{ij} is the intensity of the emission due to

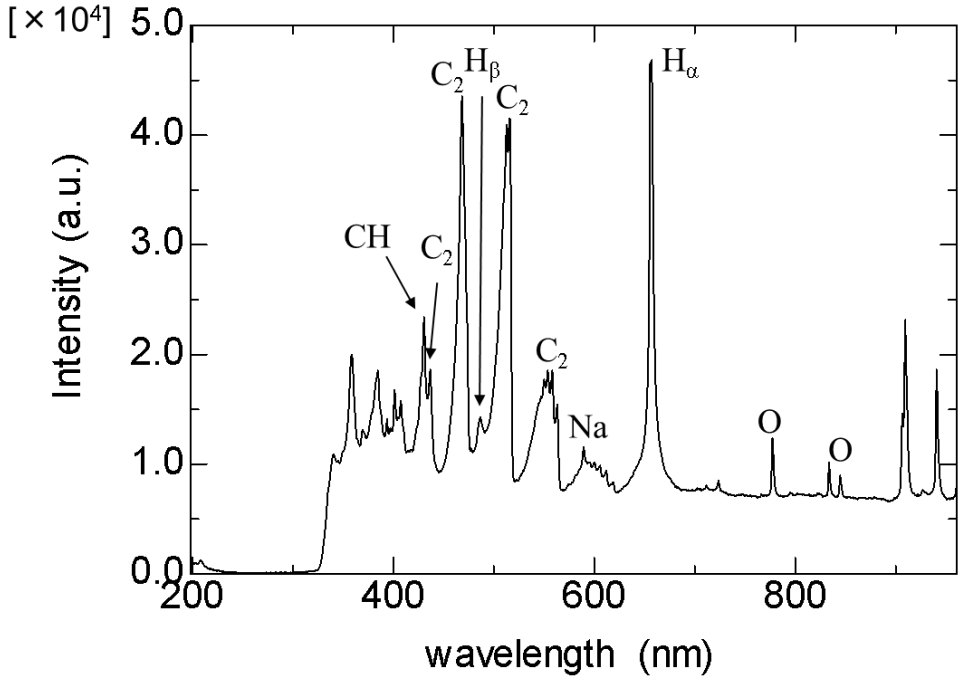

Fig. 5-9. Emission spectrum of plasma generated in acetone at 351 W discharge power

the transition from the energy level *i* to the energy level *j*, ν_{ij} is the frequency of a spectral line, A_{ij} is the Einstein A coefficient (transition probability) and g_i is the statistical weight of the energy levels. The excitation temperature was estimated to be in the range of about 3600 to 4600 K at each discharge power. The variation of the electron temperature is considered to be due to the strong light emission of C_2 near the light emission of H_β.

5- 3 - 6 Decomposition mechanism of acetone

It has been reported that plasma was generated in water under similar conditions (radio frequency, in atmospheric pressure, at 210 W power). The plasma density was 2.5×10^{20} m^{-3}, and both plasma and excitation temperatures were estimated to be approximately 4500 K [55]. It suggest that the radio

frequency in-liquid plasma at atmospheric pressure is at or near thermal equilibrium, and note that the plasma temperature is close to the electron temperature (3600 to 4600 K) in this experiment.

In the high-temperature plasma, acetone is pyrolyzed, and dissociation by electron collision occurs. Reactions (1)-(4) are considered to be principal reactions because CO is the main generated gas.

$CH_3COCH_3 \rightarrow CH_3CO + CH_3$ (1)

$CH_3COCH_3 + e \rightarrow CH_3CO + CH_3 + e$ (2)

$CH_3CO \rightarrow CO + CH_3$ (3)

$CH_3CO + e \rightarrow CO + CH_3 + e$ (4)

Note that radical and thermal decomposition reactions occur via complex mechanisms in the plasma; however, potential reactions from the product results and literature data on reaction kinetics are proposed in Table 5-2. Here, data for the rate constant of each reaction was referenced from the NIST data base [112]. However, since the recommended temperature is less than 3600 K in many reactions, the accuracy is insufficient. The rate constant k of the reaction is defined as follows:

$k = A(T/298\,K)^n exp(-E_a/RT)$

where A is the frequency factor, E_a is activation energy, R is the universal gas constant, and T is temperature.

CH_3 radicals generated in Reactions (1)-(4) are further decomposed in the plasma, and their decomposition products are also involved in the reaction such that H_2, CH_4, C_2H_2, C_2H_4, C_2H_6, and C are produced (No.7-No.15, No.17, No.20-No.26, and No.28-No.30). C atoms and C molecules are graphitized under the high temperature of 3500 K. However, as described in Section 5-3-2, at a point away from the tip of the electrode, the temperature drops rapidly and carbon is not fully carbonized and the crystallinity is low. As shown in Table 5-1, benzene, diacetylene, and diketene emissions are confirmed. Acetylene, ethylene, and ketene are polymerized in the plasma, respectively. It is considered that the acetic anhydride and triacetyl methane shown in Table 1 are produced by dehydration condensation of the acetic acid and the reaction of acetone and the CH_3CO, radical, respectively. The

production of CO_2 and acetic acid suggests that the O radical or OH radical are generated in the plasma. Although the O radical is generated by dissociation of CO (No.31), the O radical is also generated by dissociation of water slightly contained in the acetone reagent (No.34).

Table. 5-2. Potential reactions when acetone is decomposed by plasma[112]

No.	Reaction	A	n	E_a
1	$CH_3COCH_3 \rightarrow CH_3CO + CH_3$	1.1×10^{16}	0	342
2	$CH_3COCH_3 + H \rightarrow H_2 + CH_3COCH_2$	3.9×10^{-13}	0	0
3	$CH_3COCH_3 + O \rightarrow OH + CH_3COCH_2$	1.0×10^{-21}	3.71	10.7
4	$CH_3COCH_3 + OH \rightarrow CH_3COOH + CH_3$	1.00×10^{-14}	0	14.64
5	$CH_3CO \rightarrow CO + CH_3$	3.87×10^{13}	0.63	70.7
6	$CH_3CO \rightarrow CH_2CO + H$	8.74×10^{12}	1.94	192
7	$CH_3 \rightarrow H + CH_2$	1.1	0	459
8	$CH_3 + H \rightarrow CH_4$	3.2×10^{-10}	0	1.2
9	$CH_3 + H \rightarrow CH_2 + H_2$	1.0×10^{-10}	0	63.2
10	$CH_3 + CH_2 \rightarrow C_2H_4 + H$	7.01×10^{-11}	0	0
11	$CH_3 + CH_3 \rightarrow C_2H_6$	5.99×10^{-11}	0	0
12	$CH_3 + CH_3 \rightarrow C_2H_4 + H_2$	1.66×10^{-8}	0	134
13	$CH_2 \rightarrow CH + H$	6.6×10^{-9}	0	348
14	$CH_2 \rightarrow H_2 + C$	2.7×10^{-10}	0	268
15	$CH_2 + CH_2 \rightarrow C_2H_2 + H_2$	2.62×10^{-9}	0	50
16	$CH_2 + O \rightarrow CO + H_2$	2.0×10^{-10}	0	0
17	$CH_2 + H \rightarrow CH + H_2$	1.0×10^{-11}	0	0.9

18	**$CH + O \rightarrow CO + H$**	**2.1×10^{-10}**	**0**	**0**
19	**$CH + O \rightarrow C + OH$**	**2.5×10^{-11}**	**0**	**198**
20	**$CH + H \rightarrow C + H_2$**	**1.3×10^{-10}**	**0**	**66.5**
21	**$C_2H_6 + CH_3 \rightarrow CH_4 + C_2H_5$**	**7.19×10^{-15}**	**4**	**34.67**
22	**$C_2H_5 + CH_3CO \rightarrow CH_3COC_2H_5$**	**3.01×10^{-15}**	**-0.5**	**0**
23	**$C_2H_4 + H \rightarrow C_2H_5$**	**6.79×10^{-12}**	**1.49**	**4.15**
24	**$C_2H_4 + H_2 \rightarrow C_2H_6$**	**1.83×10^{-21}**	**0**	**0**
25	**$C_2H_2 \rightarrow C_2 + H_2$**	**7.6×10^{-17}**	**0**	**17.2**
26	**$C_2H_2 \rightarrow C_2H + H$**	**6.64×10^{-8}**	**0**	**447**
27	**$C_2H_2 + O \rightarrow CO + CH_2$**	**2.0×10^{-10}**	**0**	**3.3**
28	**$C_2H_2 + H \rightarrow C_2H + H_2$**	**1.0×10^{-10}**	**0**	**116**
29	**$C_2H_2 + C_2H \rightarrow C_4H_2 + H$**	**1.25×10^{-10}**	**0**	**0**
30	**$C_2H + H \rightarrow C_2 + H_2$**	**5.99×10^{-11}**	**0**	**118**
31	**$CO \rightarrow C + O$**	**1.52×10^{-4}**	**-3.1**	**1073**
32	**$CO + O \rightarrow CO_2$**	**1.6×10^{-14}**	**0**	**8.1**
33	**$CO + OH \rightarrow CO_2 + H$**	**3.5×10^{-12}**	**0**	**21.9**
34	**$H_2O \rightarrow OH + H$**	**6.56×10^{-10}**	**0**	**446**

5 – 3 Conclusions

In this study, we obtained hydrogen energy and two types of solid carbon by decomposing acetone using plasma while suppressing the generation of CO_2. The energy efficiencies of the acetone decomposition and hydrogen production reached approximately 0.9 $\mu molJ^{-1}$ and 1.0 $\mu molJ^{-1}$ at a discharge power of 407 W. GCMS analysis confirmed the production of undesirable organic matter, such as benzene. Carbon dispersed in the liquid and carbon extending from the electrode were confirmed, which are considered to have been generated in the region where the plasma temperature differed. Elemental analysis and Raman spectroscopic analysis confirm that stick carbon extending from the electrode contained lower ratio of oxygen and hydrogen and has higher crystallinity than powdery carbon dispersed in the solution.

Chapter 6. General conclusion

In this study, in-liquid plasma was applied to the decomposition of biomass and waste solvents. The results of detailed examination of its usefulness from the viewpoint of decomposition efficiency and by-products produced were summarized. Cellulose and lignin, which are the main components of forest land remaining materials, and acetone, which is often used as an organic solvent, were targeted for decomposition.

In Chapter 1, the research on the characteristics of plasma in liquid and its application was outlined. In addition, the research background was described from the advantages of decomposing biomass and waste solvents by in-liquid plasma, and the relationship between global resource demand and the earth's regenerative capacity.

In Chapter 2 and 3, the influence of electrolyte concentration on cellulose decomposition was investigated, and the relationship between plasma size and gas temperature and gas production rate was summarized. As a result of using pure water and electrolyte solutions as cellulose dispersions, it was found that the plasma temperature did not depend on the electrolyte concentration, but the plasma size increased with the electrolyte concentration, and the gas generation rate increased. In addition, by measuring the hydrogen peroxide concentration after plasma irradiation, it was considered that OH radicals contributed to the cellulose decomposition reaction.

In Chapter 4, the attempt was made to generate aromatic hydrocarbons simultaneously with synthesis gas by decomposing a solution of lignin in methanol by in-liquid plasma. As a result, we succeeded in producing gases with hydrogen and carbon monoxide as main components and aromatic hydrocarbons such as benzene and toluene. It was found that the production rate of aromatic hydrocarbons increased with the concentration of lignin in the solution, but the production rate of hydrogen and carbon monoxide decreased. The lignin that could not be decomposed was confirmed as deposits on the electrode, suggesting that this interfered with the discharge.

In Chapter 5, the attempt was made to generate syngas and carbon material simultaneously by decomposing acetone as a waste solvent model by in-liquid plasma. By conducting Raman spectroscopy and elemental analysis, it was clarified that two kinds of carbon materials with different crystallinity were produced by plasma decomposition. It can be used as a carbon material, and future development is expected. In addition, the mechanism of decomposition was discussed by referring to the reaction kinetic database based on the results of plasma emission spectroscopy.

It was revealed that fuel gas can be generated from biomass and waste solution by using in-liquid plasma. However, since much of the plasma energy is consumed for increasing the liquid temperature, the energy efficiency of the hydrogen generation is less than the electrolysis of water. Therefore, in order to use in-liquid plasma as a method for decomposing organic substances, it is necessary to add value other than the production of fuel gas. In this study, the generation of aromatic compounds and carbon materials was confirmed when biomass and waste solvents were decomposed. It is expected that further establishment of the utilization of by-products generated in the processing by the in-liquid plasma will be effective utilization of the total energy, and will be closer to practical use. These studies provide important knowledge about the production of hydrogen and valuable materials by organic matter decomposition using in-liquid plasma method.

Reference

[1] Nomura S, Toyota H. Sonoplasma generated by a combination of ultrasonic waves and microwave irradiation. Appl Phys Lett 2003;83:4503–5. doi:10.1063/1.1631062.

[2] Maehara T, Toyota H, Kuramoto M, Iwamae A, Tadokoro A, Mukasa S, et al. Radio frequency plasma in water. Japanese J Appl Physics, Part 1 (Regular Pap Short Notes & Rev Pap 2006;45:8864–8. doi:10.1143/JJAP.45.8864.

[3] Hattori Y, Mukasa S, Toyota H, Inoue T, Nomura S. Synthesis of zinc and zinc oxide nanoparticles from zinc electrode using plasma in liquid. Mater Lett 2011;65:188–90. doi:10.1016/j.matlet.2010.09.068.

[4] Hattori Y, Mukasa S, Toyota H, Inoue T, Nomura S. Continuous synthesis of magnesium-hydroxide, zinc-oxide, and silver nanoparticles by microwave plasma in water. Mater Chem Phys 2011;131:425–30. doi:10.1016/j.matchemphys.2011.09.068.

[5] Hattori Y, Nomura S, Mukasa S, Toyota H, Inoue T. Synthesis of tungsten trioxide nanoparticles by microwave plasma in liquid and analysis of physical properties. J Alloys Compd 2013;560:105–10.

[6] Hattori Y, Nomura S, Mukasa S, Toyota H, Inoue T, Usui T. Synthesis of tungsten oxide, silver, and gold nanoparticles by radio frequency plasma in water. J Alloys Compd 2013;578:148–52. doi:10.1016/j.jallcom.2013.05.032.

[7] Amaliyah N, Mukasa S, Nomura S, Toyota H. Plasma In-liquid Method for Reduction of Zinc Oxide in Zinc Nanoparticle Synthesis. Mater Res Express 2015;2:25004. doi:10.1088/2053-1591/2/2/025004.

[8] MUKASA S, UDAKA Y, MATSUZAWA K, DOI N, TOYOTA H, NOMURA S. Effect of Reduction Agent on ZnO Reduction by Radio-frequency Dielectric Heating. J Japan Inst Energy 2017;96:357–61. doi:10.3775/jie.96.357.

[9] Syahrial F, Mukasa S, Toyota H, Okamoto K, Nomura S. Hydrogen production from glucose and cellulose using radio frequency in-liquid plasma and ultrasonic irradiation. Nihon Enerugi Gakkaishi/Journal Japan Inst Energy 2014;93:1207–12.

[10] Nomura S, Toyota H, Mukasa S, Yamashita H, Maehara T, Kawashima A. Production of hydrogen in a conventional microwave oven. J Appl Phys 2009;106:1–4. doi:10.1063/1.3236575.

[11] Shiraishi R, Nomura S, Mukasa S, Nakano R, Kamatoko R. Effect of catalytic electrode and plate for methanol decomposition by in-liquid plasma. Int J Hydrogen Energy 2018;43. doi:10.1016/j.ijhydene.2018.01.060.

[12] Shiraishi R, Nomura S, Toyota H, Mukasa S. Effect of introducing a steam pipe to n- dodecane decomposition by in-liquid plasma for hydrogen production. Int J Hydrogen Energy 2019;44:16248–56.

[13] Iyengar L, Jeffries B, Oerlemans N. Living Planet Report 2014:species and spaces, people and places. 2014.

[14] Sasaki M, Kabyemela B, Malaluan R, Hirose S, Takeda N, Adschiri T, et al. Cellulose hydrolysis in subcritical and supercritical water. J Supercrit Fluids 1998;13:261–8. doi:10.1016/S0896-8446(98)00060-6.

[15] El-Zawawy WK, Ibrahim MM, Abdel-Fattah YR, Soliman NA, Mahmoud MM. Acid and enzyme hydrolysis to convert pretreated lignocellulosic materials into glucose for ethanol production. Carbohydr Polym 2011;84:865–71. doi:10.1016/j.carbpol.2010.12.022.

[16] Hamelinck CN, Van Hooijdonk G, Faaij APC. Ethanol from lignocellulosic biomass: Techno-economic performance in short-, middle- and long-term. Biomass and Bioenergy 2005;28:384–410. doi:10.1016/j.biombioe.2004.09.002.

[17] Banerjee S, Mudliar S, Sen R, Giri B, Satpute D, Chakrabarti T, et al. Commercializing lignocellulosic bioethanol: technology bottlenecks and possible remedies. Biofuels, Bioprod Biorefining 2009;4:77–93. doi:10.1002/bbb.

[18] Liu H, Sun J, Leu S-Y, Chen S. Toward a fundamental understanding of cellulase-lignin interactions in the whole slurry enzymatic saccharifi cation process. Biofuels, Bioprod Biorefining 2016;10:648–63. doi:10.1002/bbb.

[19] Pu Y, Hu F, Huang F, Ragauskas AJ. Lignin Structural Alterations in Thermochemical Pretreatments with Limited Delignification. Bioenergy Res 2015;8:992–1003. doi:10.1007 /s12155-015-9655-5.

[20] Chen L, Fu S. Enhanced cellulase hydrolysis of eucalyptus waste fibers from pulp mill by tween80-assisted ferric chloride pretreatment. J Agric Food Chem 2013;61:3293–300. doi:10.1021/jf400062e.

[21] Hendriks ATWM, Zeeman G. Pretreatments to enhance the digestibility of lignocellulosic biomass. Bioresour Technol 2009;100:10–8. doi:10.1016/j.biortech.2008.05.027.

[22] Nomura S, Miyagawa S, Mukasa S, Toyota H. Decomposition of cellulose by ultrasonic welding in water. Jpn J Appl Phys 2016;55:7–8. doi:10.7567/JJAP.55.07KE02.

[23] Changsuwan P, Paksung N, Inoue S, Inoue T, Kawai Y, Noguchi T, et al. Conversion of guaiacol in supercritical water gasification: Detailed effect of feedstock concentration. J Supercrit Fluids 2018;142:32–7. doi:10.1016/j.supflu.2018.05.024.

[24] Paksung N, Kato J, Nakashimada Y, Matsumura Y. Process design and evaluation of supercritical water gasification of tomato residue in a rural area of Japan. J Japan Pet Inst 2018;61:213–8. doi:10.1627/jpi.61.213.

[25] Yoshida T, Matsumura Y. Gasification of cellulose, xylan, and lignin mixtures in supercritical water. Ind Eng Chem Res 2001;40:5469–74. doi:10.1021/ie0101590.

[26] Chun YN, Kim EH, Lim MS, Cheon W Il. Development of a Plasma-Dump Combustor for VOC Destruction. Appl Mech Mater 2015;789–790:436–40. doi:10.4028/www.scientific.net/amm. 789-790.436.

[27] Oda T. Non-thermal plasma processing for environmental proection: Decomposition of dilute VOCs in air. J Electrostat 2003;57:293–311. doi:10.1016/S0304-3886(02)00179-1.

[28] Wu JCS, Chang TY. VOC deep oxidation over Pt catalysts using hydrophobic supports. Catal Today 1998;44:111–8. doi:10.1016/s0920-5861(98)00179-5.

[29] Cordi EM, O'Neill PJ, Falconer JL. Transient oxidation of volatile organic compounds on a CuO/AL2O3 catalyst. Appl Catal B Environ 1997;14:23–36. doi:10.1016/S0926-3373(97)00009-X.

[30] Parida KM, Samal A. Catalytic combustion of volatile organic compounds on Indian Ocean manganese nodules. Appl Catal A Gen 1999;182:249–56. doi:10.1016/S0926-860X(99)00015-0.

[31] Verykios XE, Papaefthimiou P, Ioannides T. Combustion of non-halogenated volatile organic compounds over group VIII metal catalysts. Appl Catal B Environ 1997;13:175–84.

[32] Zhang C, Cao Z, Lu Y, Du L. Research on Influencing Factors of Biological Filtration Tower Treating Toluene Gas. IOP Conf Ser Earth Environ Sci 2017;63. doi:10.1088/1755-1315/63/1/012020.

[33] Aizpuru A, Khammar N, Malhautier L, Fanlo JL. Biofiltration for the treatment of complex mixtures of VOC influence of the packing material. Acta Biotechnol 2003;23:211–26. doi:10.1002/abio.200390027.

[34] Daubert I, Lafforgue C, Maranges C, Fonade C. Feasibility study of a compact process for biological treatment of highly soluble VOCs polluted gaseous effluent. Biotechnol Prog 2001;17:1084–92. doi:10.1021/bp010094w.

[35] Pak SH, Jeon MJ, Jeon YW. Study of sulfuric acid treatment of activated carbon used to enhance mixed VOC removal. Int Biodeterior Biodegrad 2016;113:195–200. doi:10.1016/j.ibiod. 2016.04.019.

[36] Mohan N, Kannan GK, Upendra S, Subha R, Kumar NS. Breakthrough of toluene vapours in granular activated carbon filled packed bed reactor. J Hazard Mater 2009;168:777–81. doi:10.1016/j.jhazmat.2009.02.079.

[37] Kapdan IK, Kargi F. Bio-hydrogen production from waste materials. Enzyme Microb Technol 2006;38:569–82. doi:10.1016/j.enzmictec.2005.09.015.

[38] Nehrir MH, Wang C, Strunz K, Aki H, Ramakumar R, Bing J, et al. A review of hybrid renewable/alternative energy systems for electric power generation: Configurations, control, and applications. IEEE Trans Sustain Energy 2011;2:392–403. doi:10.1109/TSTE.2011.2157540.

[39] Ashok B, Thundil Karuppa Raj R, Nanthagopal K, Krishnan R, Subbarao R. Lemon peel oil – A novel renewable alternative energy source for diesel engine. Energy Convers Manag 2017;139:110–21. doi:10.1016/j.enconman.2017.02.049.

[40] A.B.M SH, Aishah S. Biodiesel Fuel Production from Algae as Renewable Energy. Am J Biochem Biotechnol 2008;4:250–4.

[41] Florin N, Harris A. Hydrogen production from biomass. Environmentalist 2007;27:207–15. doi:10.1007/s10669-007-9027-6.

[42] Saidur R, Abdelaziz EA, Demirbas A, Hossain MS, Mekhilef S. A review on biomass as a fuel for boilers. Renew Sustain Energy Rev 2011;15:2262–89. doi:10.1016/j.rser.2011.02.015.

[43] Demirbaş A. Biomass resource facilities and biomass conversion processing for fuels and chemicals. Energy Convers Manag 2001;42:1357–78. doi:10.1016/S0196-8904(00)00137-0.

[44] McKendry P. Energy production from biomass (part 1): overview of biomass. Bioresour Technol 2002;83:37–46. doi:10.1016/S0960-8524(01)00118-3.

[45] McKendry P. Energy production from biomass (part 2): conversion technologies. Bioresour Technol 2002;83:47–54. doi:10.1016/S0960-8524(01)00119-5.

[46] Saxena RC, Seal D, Kumar S, Goyal HB. Thermo-chemical routes for hydrogen rich gas from biomass: A review. Renew Sustain Energy Rev 2008;12:1909–27. doi:10.1016/j.rser. 2007.03.005.

[47] Han J, Kim H. The reduction and control technology of tar during biomass gasification/pyrolysis: An overview. Renew Sustain Energy Rev 2008;12:397–416. doi:10.1016/j.rser.2006.07.015.

[48] Zhang L, Xu C (Charles), Champagne P. Overview of recent advances in thermo-chemical conversion of biomass. Energy Convers Manag 2010;51:969–82. doi:10.1016/j.enconman. 2009.11.038.

[49] Tao X, Bai M, Li X, Long H, Shang S, Yin Y, et al. CH4–CO2 reforming by plasma – challenges and opportunities. Prog Energy Combust Sci 2011;37:113–24. doi:10.1016/j.pecs.2010.05.001.

[50] Henriques J, Bundaleska N, Tatarova E, Dias FM, Ferreira CM. Microwave plasma torches driven by surface wave applied for hydrogen production. Int J Hydrogen Energy 2011;36:345–54. doi:10.1016/j.ijhydene.2010.09.101.

[51] Sun B, Sato M, Harano A, Clements J. Non-uniform pulse discharge-induced radical production in distilled water. J Electrostat 1998;43:115–26. doi:10.1016/S0304-3886(97)00166-6.

[52] Sugiarto AT, Sato M. Pulsed plasma processing of organic compounds in aqueous solution. Thin Solid Films 2001;386:295–9. doi:10.1016/S0040-6090(00)01669-2.

[53] Nomura S, Toyota H, Mukasa S, Takahashi Y, Maehara T, Kawashima A, et al. Discharge characteristics of microwave and high-frequency in-liquid plasma in water. Appl Phys Express 2008;1:0460021–3. doi:10.1143/APEX.1.046002.

[54] Mukasa S, Nomura S, Toyota H, Maehara T, Abe F, Kawashima A. Temperature distributions of radio-frequency plasma in water by spectroscopic analysis. J Appl Phys 2009;106:1–6. doi:10.1063/1.3264671.

[55] Maehara T, Honda S, Inokuchi C, Kuramoto M, Mukasa S, Toyota H, et al. Influence of conductivity on the generation of a radio frequency plasma surrounded by bubbles in water. Plasma Sources Sci Technol 2011;20:034016. doi:10.1088/0963-0252/20/3/034016.

[56] He Y, Pang Y, Liu Y, Li X, Wang K. Physicochemical characterization of rice straw pretreated with sodium hydroxide in the solid state for enhancing biogas production. Energy and Fuels 2008;22:2775–81. doi:10.1021/ef8000967.

[57] Syahrial F, Nomura S, Mukasa S, Toyota H, Okamoto K. Synergetic effects of radio-frequency (RF) in-liquid plasma and ultrasonic vibration on hydrogen production from glucose. Int J Hydrogen Energy 2015;40:11399–405. doi:10.1016/j.ijhydene.2015.04.152.

[58] Brethauer S, Wyman CE. Review: Continuous hydrolysis and fermentation for cellulosic ethanol production. Bioresour Technol 2010;101:4862–74. doi:10.1016/j.biortech.2009.11.009.

[59] Kazi FK, Patel AD, Serrano-Ruiz JC, Dumesic JA, Anex RP. Techno-economic analysis of dimethylfuran (DMF) and hydroxymethylfurfural (HMF) production from pure fructose in catalytic processes. Chem Eng J 2011;169:329–38. doi:10.1016/j.cej.2011.03.018.

[60] Zhou J, Zhang L. Solubility of cellulose in NaOH / urea aqueous solution. Polym J n.d.;32:866–70.

[61] Chundawat SPS, Bellesia G, Uppugundla N, Sousa C, Gao D, Cheh AM, et al. Restructuring the Crystalline Cellulose Hydrogen Bond Network Enhances Its Depolymerization Rate. J Am Chem Soc 2011;133:11163–74. doi:10.1021/ja2011115.

[62] Sato K, Yasuoka K, Ishii S. Water treatment with pulsed discharges generated inside bubbles. Electr Eng Japan (English Transl Denki Gakkai Ronbunshi) 2010;170:1–7. doi:10.1002/eej.20918.

[63] Li J, Sato M, Ohshima T. Degradation of phenol in water using a gas-liquid phase pulsed discharge plasma reactor. Thin Solid Films 2007;515:4283–8. doi:10.1016/j.tsf.2006.02.070.

[64] Inaba T, Iwao T. Treatment of waste by dc arc discharge plasmas. IEEE Trans Dielectr Electr Insul 2000;7:684–92. doi:10.1109/94.879362.

[65] Figueroa E, Fuentes V. Generation of electricity and waste management by using plasma. J Phys Conf Ser 2018;1043. doi:10.1088/1742-6596/1043/1/012065.

[66] Gao Y, Uner NB, Thimsen E, Foston MB. Accessing unconventional biofuels via reactions far from local equilibrium. Fuel 2018;226:472–8. doi:10.1016/j.fuel.2018.03.188.

[67] Nomura S, Mukasa S, Toyota H, Miyake H, Yamashita H, Maehara T, et al. Characteristics of in-liquid plasma in water under higher pressure than atmospheric pressure. Plasma Sources Sci Technol 2011;20:34012. doi:10.1088/0963-0252/20/3/034012.

[68] Maehara T, Miyamoto I, Kurokawa K, Hashimoto Y, Iwamae A, Kuramoto M, et al. Degradation of methylene blue by RF plasma in water. Plasma Chem Plasma Process 2008;28:467–82. doi:10.1007/s11090-008-9142-2.

[69] Mukasa S, Nomura S, Toyota H. Measurement of temperature in sonoplasma. Japanese J Appl Physics, Part 1 Regul Pap Short Notes Rev Pap 2004;43:2833–7. doi:10.1143/JJAP.43.2833.

[70] Nomura S, Toyota H, Mukasa S, Yamashita H, Maehara T, Kuramoto M. Microwave plasma in hydrocarbon liquids. Appl Phys Lett 2006;88:114–6. doi:10.1063/1.2208167.

[71] Putra AEE, Nomura S, Mukasa S, Toyota H. Hydrogen production by radio frequency plasma stimulation in methane hydrate at atmospheric pressure. Int J Hydrogen Energy 2012;37:16000–5. doi:10.1016/j.ijhydene.2012.07.099.

[72] Rahim I, Nomura S, Mukasa S, Toyota H, Kawanishi K, Makiura Y, et al. Fuel Gas Production from Biomass Sources by Radio Frequency In-Liquid Plasma Method. J Power Energy Eng 2015;03:28–35. doi:10.4236/jpee.2015.38004.

[73] Lalaurette E, Thammannagowda S, Mohagheghi A, Maness PC, Logan BE. Hydrogen production from cellulose in a two-stage process combining fermentation and electrohydrogenesis. Int J Hydrogen Energy 2009;34:6201–10. doi:10.1016/j.ijhydene. 2009.05.112.

[74] Abbas HF, Wan Daud WMA. Hydrogen production by methane decomposition: A review. Int J Hydrogen Energy 2010;35:1160–90. doi:10.1016/j.ijhydene.2009.11.036.

[75] Alvarez-Galvan MC, Mota N, Ojeda M, Rojas S, Navarro RM, Fierro JLG. Direct methane conversion routes to chemicals and fuels. Catal Today 2011;171:15–23. doi:10.1016/j.cattod. 2011.02.028.

[76] Joensen F, Rostrup-Nielsen JR. Conversion of hydrocarbons and alcohols for fuel cells. J Power Sources 2002;105:195–201. doi:10.1016/S0378-7753(01)00939-9.

[77] Xu J, Froment GF. Methane steam reforming, methanation and water-gas shift: I. Intrinsic kinetics. AIChE J 1989;35:88–96. doi:10.1002/aic.690350109.

[78] Kobayashi Y, Kosaka K, Yamamoto T, Tachikawa Y, Ito K, Sasaki K. A solid polymer water electrolysis system utilizing natural circulation. Int J Hydrogen Energy 2014;39:16263–74. doi:10.1016/j.ijhydene.2014.07.153.

[79] Nozaki T, Okazaki K. Non-thermal plasma catalysis of methane: Principles, energy efficiency, and applications. Catal Today 2013;211:29–38. doi:10.1016/j.cattod.2013.04.002.

[80] Nozaki T, Tsukijihara H, Fukui W, Okazaki K. Kinetic analysis of the catalyst and nonthermal plasma hybrid reaction for methane steam reforming. Energy and Fuels 2007;21:2525–30. doi:10.1021/ef070117+.

[81] Kameshima S, Tamura K, Ishibashi Y, Nozaki T. Pulsed dry methane reforming in plasma-enhanced catalytic reaction. Catal Today 2015;256:67–75. doi:10.1016/j.cattod.2015.05.011.

[82] Syahrial F, Mukasa S, Toyota H, Okamoto K. Hydrogen Production from Glucose and Cellulose Using Radio Frequency In-Liquid Plasma and Ultrasonic Irradiation. J Japan Inst Energy 2014;93:1207–12.

[83] Tange K, Nomura S, Mukasa S, Toyota H, Syahrial F. Effect of Pretreatment by Sulfuric Acid on Cellulose Decomposition Using the In-Liquid Plasma Method. J Japan Inst Energy 2016;95:1105–9.

[84] Luque J, Crosley D. LIFBASE (version 1.5). SRI Int Rep MP 1999;99:19.

[85] Shih KY, Locke BR. Effects of electrode protrusion length, pre-existing bubbles, solution conductivity and temperature, on liquid phase pulsed electrical discharge. Plasma Process Polym 2009;6:729–40. doi:10.1002/ppap.200900044.

[86] Mukasa S, Nomura S, Toyota H, Maehara T, Yamashita H. Internal conditions of a bubble containing radio-frequency plasma in water. Plasma Sources Sci Technol 2011;20:034020. doi:10.1088/0963-0252/20/3/034020.

[87] Amen-chen C, Pakdel H, Roy C. Production of monomeric phenols by thermochemical conversion of biomass : a review 2001;79.

[88] Takada D, Ehara K, Saka S. Gas chromatographic and mass spectrometric (GC-MS) analysis of lignin-derived products from Cryptomeria japonica treated in supercritical water. J Wood Sci 2004;50:253–9. doi:10.1007/s10086-003-0562-6.

[89] Zhao J, Xiuwen W, Hu J, Liu Q, Shen D, Xiao R. Thermal degradation of softwood lignin and hardwood lignin by TG- FTIR and Py-GC / MS. Polym Degrad Stab 2014;108:133–8. doi:10.1016/j.polymdegradstab.2014.06.006.

[90] Ehara K, Takada D, Saka S. GC-MS and IR spectroscopic analyses of the lignin-derived products from softwood and hardwood treated in supercritical water. J Wood Sci 2005;51:256–61. doi:10.1007/s10086-004-0653-z.

[91] Ponomarev A V. Radiolysis of lignin : Prospective mechanism of high-temperature decomposition. Radiat Phys Chem 2017;141:160–7. doi:10.1016/j.radphyschem.2017.07.007.

[92] Saisu M, Sato T, Watanabe M, Adschiri T, Arai K. Conversion of lignin with supercritical water-phenol mixtures. Energy and Fuels 2003;17:922–8. doi:10.1021/ef0202844.

[93] Fang Z, Sato T, Smith RL, Inomata H, Arai K, Kozinski JA. Reaction chemistry and phase behavior of lignin in high-temperature and supercritical water. Bioresour Technol 2008;99:3424–30. doi:10.1016/j.biortech.2007.08.008.

[94] Nomura S, Toyota H, Tawara M, Yamashita H, Matsumoto K. Fuel gas production by microwave plasma in liquid. Appl Phys Lett 2006;88:114–6. doi:10.1063/1.2210448.

[95] Park H, Choi W. Photocatalytic conversion of benzene to phenol using modified TiO 2 and polyoxometalates 2005;101:291–7. doi:10.1016/j.cattod.2005.03.014.

[96] Fujishima K, Fukuoka A, Yamagishi A, Inagaki S. Photooxidation of benzene to phenol by ruthenium bipyridine complexes grafted on mesoporous silica FSM-16 2001;166:211–8.

[97] Kalabokas PD, Hatzianestis J, Bartzis JG, Papagiannakopoulos P. Atmospheric concentrations of saturated and aromatic hydrocarbons around a Greek oil refinery. Atmos Environ 2001;35:2545–55. doi:10.1016/S1352-2310(00)00423-4.

[98] Tiwari V, Hanai Y, Masunaga S. Ambient levels of volatile organic compounds in the vicinity of petrochemical industrial area of Yokohama , Japan 2010:65–75. doi:10.1007/s11869-009-0052-0.

[99] Kume K, Ohura T, Amagai T, Fusaya M. Field monitoring of volatile organic compounds using passive air samplers in an industrial city in Japan. Environ Pollut 2008;153:649–57. doi:10.1016/j.envpol.2007.09.023.

[100] Centeno MA, Paulis M, Montes M, Odriozola JA. Catalytic combustion of volatile organic compounds on Au / CeO 2 / Al 2 O 3 and Au / Al 2 O 3 catalysts 2002;234:65–78.

[101] Zhou G, He X, Liu S, Xie H, Fu M. Phenyl VOCs catalytic combustion on supported CoMn/AC oxide catalyst. J Ind Eng Chem 2015;21:932–41. doi:10.1016/j.jiec.2014.04.035.

[102] Estrada JM, Bernal OI, Flickinger MC, Muñoz R, Deshusses MA. Biocatalytic coatings for air pollution control: A proof of concept study on VOC biodegradation. Biotechnol Bioeng 2015;112:263–71. doi:10.1002/bit.25353.

[103] Sultana S, Vandenbroucke A, Leys C, De Geyter N, Morent R. Abatement of VOCs with Alternate Adsorption and Plasma-Assisted Regeneration: A Review. Catalysts 2015;5:718–46. doi:10.3390/catal5020718.

[104] Su J, Bae J, Park S, Park Y. Plasma-assisted oxidation of toluene over Fe / zeolite catalyst in DBD reactor using adsorption / desorption system. Catal Commun 2018;113:36–40. doi:10.1016/j.catcom.2018.05.013.

[105] Shang K, Zhao Z, Zhou X, Wang X. Design of a Novel Corona Plasma Reactor for Decomposition of VOCs 2010;114:146–9. doi:10.4028/www.scientific.net/AMR.113-116.146.

[106] Vandenbroucke AM, Morent R, Geyter N De, Leys C. Non-thermal plasmas for non-catalytic and catalytic VOC abatement. J Hazard Mater 2011;195:30–54. doi:10.1016/j.jhazmat.2011.08.060.

[107] Chang C, Lin T. Decomposition of Toluene and Acetone in Packed Dielectric Barrier Discharge Reactors. Plasma Chem Plasma Process 2005;25:227–43. doi:10.1007/s11090-004-3034-x.

[108] Soucy SSG. Liquid and solution treatment by thermal plasma : a review. Int J Environ Sci Technol 2013;11:1165–88. doi:10.1007/s13762-013-0356-3.

[109] Narengerile, Watanabe T. Acetone decomposition by water plasmas at atmospheric pressure. Chem Eng Sci 2012;69:296–303. doi:10.1016/J.CES.2011.10.045.

[110] Morishita T, Ueno T, Panomsuwan G, Hieda J, Yoshida A, Bratescu MA, et al. Fastest Formation Routes of Nanocarbons in Solution Plasma Processes. Nat Publ Gr 2016:1–13. doi:10.1038/srep36880.

[111] Wang V, Alsmeyer DC, Mccreery RL. Raman Spectroscopy of Carbon Materials : Structural Basis of Observed Spectra. Chem Mater 1990;2:557–63. doi:10.1021/cm00011a018.

[112] NIST database. Http://WebbookNistGov n.d.

Acknowledgements

This research was conducted from April 2017 to March 2020 at the Graduate School of Science and Engineering, Ehime University. Four research results were published in an international journal, and the research was presented three times at an international conference. I think that I was able to achieve such results thanks to my research in a very good environment. I thank many people who supported me.

Prof. Shinfuku Nomura taught the whole research as a supervisor, such as the focus of the research theme, how to write a paper, and how to consider. I'm really grateful for the fact that I have been doing my research because of the enthusiastic guidance.

Prof. Hiromichi Toyota gave me a lot of advice when making microwave plasma generator. I would like to thank you for taking care of the completion of the device.

Associate Professor Shinobu Mukasa taught us the knowledge necessary for research, such as emission spectra and logical calculation methods. I am grateful that this knowledge has greatly helped in my research.

Prof. Tsunehiro Maehara, Visiting Professor Junichi Nakajima, Associate Professor Yukiharu Iwamoto gave guidance in the fields of equipment, chemistry and quantum mechanics. Thank you for answering my questions.

Professor Masafumi Jinno and Associate Professor Hideki Motomura of the Department of Electrical and Electronic Engineering at this university gave us detailed information on basic knowledge of plasma engineering. Thank you for answering questions while you were busy.

Tomio Inoue, Doctor of Education, recommended me the career of a researcher. I really appreciate his many encouragements and guidance.

The reactor used in the experiment was produced at a training factory at Ehime University. I am grateful to the staff who have carefully taught me how to use machine tools.

Some chemical analyzes were conducted at Ehime Industrial Technology Research Center and Academic Support Center. I am grateful to the staff of the university and the prefecture who taught me Students from the heat and mass transfer laboratory participated in the experiment. I would like to thank for Mr. Fadhli Syahrial, Mr. Kei Okamoto, Mr. Takuma Kitahara, Mr. Yuki Nishioka, Mr. Nishio Atsuto and Mr. Inoue Rintaro. I appreciate my friends and people around me who understand and encourage me. Finally, I thank my parents for giving me birth and supporting.